

# Trait coordination and trade-offs constrain the diversity of water use strategies in Mediterranean woody plants

Received: 22 July 2024

Accepted: 18 April 2025

Published online: 02 May 2025

Francisco J. Muñoz-Gálvez<sup>1</sup>, José I. Querejeta<sup>1</sup>✉, Cristina Moreno-Gutiérrez<sup>1</sup>, Wei Ren<sup>2,3</sup>, Enrique G. de la Riva<sup>4</sup> & Iván Prieto<sup>4</sup>

The diversity of water-use strategies among dryland plants has been the focus of extensive research, but important knowledge gaps remain. Comprehensive surveys of water-use traits encompassing multiple species growing at contrasting sites are needed to further advance current understanding of plant water use in drylands. Here we show that ecohydrological niche segregation driven by differences in water uptake depth among coexisting species is widespread across Mediterranean plant communities, as evidenced by soil and stem water isotopes measured in 62 native species growing at 10 sites with contrasting climatic conditions. Foliar carbon and oxygen isotopes revealed that leaf-level stomatal regulation stringency and water-use efficiency also differ markedly among coexisting species, and are both coordinated with water uptake depth. Larger and taller woody species use a greater proportion of deeper soil water, display more conservative water use traits at leaf level (“water-savers”) and show greater investment in foliage relative to shoots. Conversely, smaller species rely mainly on shallow soil water, exhibit a more profligate water use strategy (“water-spenders”) and prioritize investment in shoots over foliage. Drought stress favours coordination between above and belowground water-use traits, resulting in unavoidable trade-offs that constrain the diversity of whole-plant water use strategies in Mediterranean plant communities.

Understanding the relationship between plant taxonomic and functional diversity has been central to ecology for decades, yet few studies have explored the potential coordination of key below- and above-ground water use traits such as soil water uptake depth by roots and leaf-level stomatal regulation stringency or water use efficiency. Plant species size and position along the Plant Economic Spectrum (acquisitive-conservative continuum) are key indicators of species nutrient and carbon use strategies<sup>1–4</sup>. However, the diversity of water use strategies among coexisting species in dryland plant communities, or the

potential coordination and tradeoffs between water uptake depth and leaf-level water use traits in drought-prone ecosystems, have received comparatively much less research attention<sup>5–10</sup>.

A generally good correlation between above and belowground plant component sizes has been described across multiple ecosystem types worldwide<sup>11</sup>. However, it is important to note that water uptake depth depends not only on plant size but also on multiple other environmental factors such as climate type or groundwater accessibility to roots<sup>12,13</sup>. In this context, plant species from humid climates

<sup>1</sup>Centro de Edafología y Biología Aplicada del Segura (CEBAS), Consejo Superior de Investigaciones Científicas, Murcia, Spain. <sup>2</sup>Institute of International Rivers and Eco-Security, Yunnan University, Kunming, China. <sup>3</sup>Chongqing Key Laboratory of Karst Environment, School of Geographical Sciences, Southwest University, Chongqing, China. <sup>4</sup>Área de Ecología, Facultad de Ciencias Biológicas y Ambientales, Departamento de Biodiversidad y Gestión Ambiental, Universidad de León, León, Spain. ✉e-mail: [querejeta@cebas.csic.es](mailto:querejeta@cebas.csic.es)

and ecosystems tend to rely more heavily on shallow soil water sources than species from dry climates, as the latter generally develop deeper root systems and are capable of using a greater proportion of deep soil/bedrock water sources<sup>12,14,15</sup>. Woody plants in Mediterranean and other dryland habitats typically use less than 30% of water from recent precipitation stored in upper soil layers<sup>16</sup>, so water uptake from deeper soil and bedrock moisture sources has an important role in sustaining vegetation transpiration during prolonged rainless periods. Vertical segregation in plant water uptake patterns among coexisting species can lead to ecohydrological niche partitioning, in which plant species with contrasting water use traits gain preferential access to different soil water pools present along the edaphic profile<sup>7</sup>. Ecohydrological niche segregation<sup>6</sup> and contrasting plant water use strategies among coexisting species and life forms could favor resource partitioning that enhances complementarity and efficiency in the use of the limited water resources in drought-prone ecosystems<sup>17</sup>.

Woody plants in seasonally dry upland Mediterranean ecosystems depend on two distinct water pools available along the edaphic profile: an easily accessible topsoil pool in upper layers with intermittent, erratic and rapidly fluctuating water availability that is recharged mainly by recent precipitation, but is exposed to rapid evaporative loss and competitive depletion by neighbors; and a less accessible, deeper soil/bedrock pool with more temporally stable water storage and availability that is recharged by large winter and autumn precipitation events and is less exposed to direct evaporative losses or competitive depletion by neighbors<sup>7,18,19</sup>. Plant species access to, and utilization of, each of these two moisture pools may be constrained by multiple trade-offs between structural and physiological traits. Traits such as small size or shallow rooting pattern may severely constrain access to the more stable water pool stored in deep soil/bedrock layers<sup>11,12,20</sup>. Whereas physiological traits associated to leaf-level water use patterns, such as stomatal regulation stringency or water use efficiency<sup>21</sup> could modulate a faster or slower utilization of the available soil water by each species according to their position along the profligate-conservative water use continuum<sup>5,22,23</sup>. Previous studies investigating the diversity of plant water use strategies present in Mediterranean plant communities largely focused on local spatial scales with relatively few coexisting species<sup>18,24,25</sup>. More ambitious and comprehensive surveys encompassing larger numbers of plant species growing at multiple sites with contrasting climatic and environmental conditions are thus needed to further advance our current understanding of water use patterns by woody vegetation across the Mediterranean biome. Moreover, such an approach could help elucidate any potential coordination and trade-offs between water uptake depth and leaf-level water use strategies across coexisting plant species and life forms at multiple sites.

Stable isotopes and their variations in plant tissues provide a valuable tool to investigate interspecific differences in water use strategies among coexisting species in natural plant communities. The isotopic composition of xylem water ( $\delta^{18}\text{O}_{\text{xw}}$ ,  $\delta^2\text{H}_{\text{xw}}$ , d-excess<sub>xw</sub>) reflects the relative proportion of water taken up from different soil depths by plants, as little or no isotopic fractionation occurs during root water uptake from soil (but see refs. 26,27 for issues with  $\delta^2\text{H}$ ). The relative contributions of shallow vs deep soil water sources to total plant water uptake can be more easily estimated when intense evaporative isotopic enrichment of the shallow soil water pool occurs<sup>28</sup>, which is typically found in Mediterranean ecosystems with frequent hot and rainless periods during which topsoil water is exposed to intense evaporative isotopic fractionation. The stable carbon isotope composition of leaf dry matter ( $\delta^{13}\text{C}_{\text{L}}$ ) represents a metabolic set point for the integration and coordination of leaf gas exchange fluxes<sup>29</sup> that is affected by both  $\text{CO}_2$  assimilation during photosynthesis and  $\text{CO}_2$  diffusion through stomata, so it provides a good proxy for time-integrated intrinsic water use efficiency ( $\text{WUE}_i$ ) defined as the ratio between net photosynthetic rate ( $A$ ) and stomatal conductance

( $g_s$ )<sup>5,21,23,30,31</sup>. The oxygen isotopic composition ( $\delta^{18}\text{O}_{\text{L}}$ ) of leaf dry matter reflects the isotopic signal of the source water used by the plant ( $\delta^{18}\text{O}_{\text{xw}}$ ), and is also affected by leaf-level evaporative effects during transpiration<sup>32,33</sup>. Thus, the oxygen isotopic composition of leaf dry matter calculated as enrichment above source water ( $\Delta^{18}\text{O}_{\text{L}} = \delta^{18}\text{O}_{\text{L}} - \delta^{18}\text{O}_{\text{xw}}$ ) can provide a time-integrated indication of cumulative  $g_s$  and transpiration over the growing season<sup>5,21</sup>. However, the interpretation of interspecific differences in  $\delta^{13}\text{C}_{\text{L}}$  and  $\Delta^{18}\text{O}_{\text{L}}$  among coexisting plant species is complicated by multiple uncertainties, due to the myriad complex factors that may affect the carbon and oxygen isotopic composition of leaf organic matter in natural plant communities<sup>30,34–39</sup>. It is thus advisable to simultaneously conduct conventional leaf gas exchange measurements (stomatal conductance, intrinsic water use efficiency) in the field to validate the interpretation of  $\delta^{13}\text{C}_{\text{L}}$  and  $\Delta^{18}\text{O}_{\text{L}}$  and to confirm that these isotopic water-use traits actually provide reliable time-integrated proxies of leaf-level water use patterns across coexisting woody species within each plant community.

In this study, we assess the diversity of plant water use strategies among coexisting woody species at ten study sites with contrasting climatic and environmental conditions in the Iberian Peninsula. Our study sites span from warm arid and semiarid areas near the Mediterranean coast where dwarf palms (*Chamaerops humilis*) and Iberian-African endemic shrubs (*Periploca angustifolia*, *Maytenus senegalensis*) are common, to much cooler and wetter areas located at higher altitudes at the Mediterranean-Temperate transitional border in central Spain, where temperate tree species such as *Fagus sylvatica* or *Quercus petraea* are present. Our 10 study sites were carefully chosen to represent the wide spectrum of precipitation and temperature conditions encountered across the Mediterranean biome (from warmer arid and semiarid climates to cooler dry-subhumid climates, Table S1). Our pool of 62 woody plant species (771 individuals) encompasses contrasting plant life forms: small shrubs (<1 m height), large shrubs (1–3 m height) and trees (3–20 m in height)<sup>11</sup>, and is representative of the large functional and taxonomic diversity of the Mediterranean biogeographical region, which includes evergreen, drought-deciduous/semideciduous and winter-deciduous species (Tables S2 and S6).

We investigate the potential occurrence of vertical niche partitioning of soil water and ecohydrological niche segregation among coexisting woody species at all the 10 study sites. Matching soil water isotopic composition variations along the soil profile with the xylem water isotopic composition of plants ( $\delta^{18}\text{O}_{\text{xw}}$ ,  $\delta^2\text{H}_{\text{xw}}$ , d-excess<sub>xw</sub>), we estimate the proportion of water taken up from shallow vs deeper moisture pools by the different species and life forms present in these plant communities during the peak of the growing season in the Mediterranean biome (Spring). In parallel, we also assess the diversity of leaf-level water use strategies using foliar  $\delta^{13}\text{C}_{\text{L}}$  and  $\Delta^{18}\text{O}_{\text{L}}$  as proxies for time-integrated water use efficiency ( $\text{WUE}_i$ ) and stomatal conductance ( $g_s$ ), respectively. In addition, we measure the leaf area to sapwood area ratio of terminal shoots as a key aboveground trait related to plant hydraulic architecture (i.e. the ratio between the total transpiring leaf area to the cross-sectional sapwood area supplying water to leaves) at two sites with contrasting climatic conditions and high plant species diversity (Yeste and Montejo, see Material and methods section). In a subset of six study sites, the isotopic water use traits of all the coexisting woody species ( $\delta^{13}\text{C}_{\text{L}}$ ,  $\Delta^{18}\text{O}_{\text{L}}$ ,  $\delta^{18}\text{O}_{\text{xw}}$ ,  $\delta^2\text{H}_{\text{xw}}$ , d-excess<sub>xw</sub>) are measured twice on two separate years (2019 and 2022) with sharply contrasting rainfall amounts and patterns, in order to assess whether interspecific differences in water use traits among coexisting species are well preserved through time across years with contrasting climatic conditions (dry vs wet years). During the second sampling year (2022) we also conduct instantaneous leaf gas exchange measurements in the field to confirm that leaf carbon and oxygen isotopes indeed provide reliable proxies of interspecific differences in leaf-level water use patterns among coexisting woody species at each study site. Finally, we investigate the potential coordination and

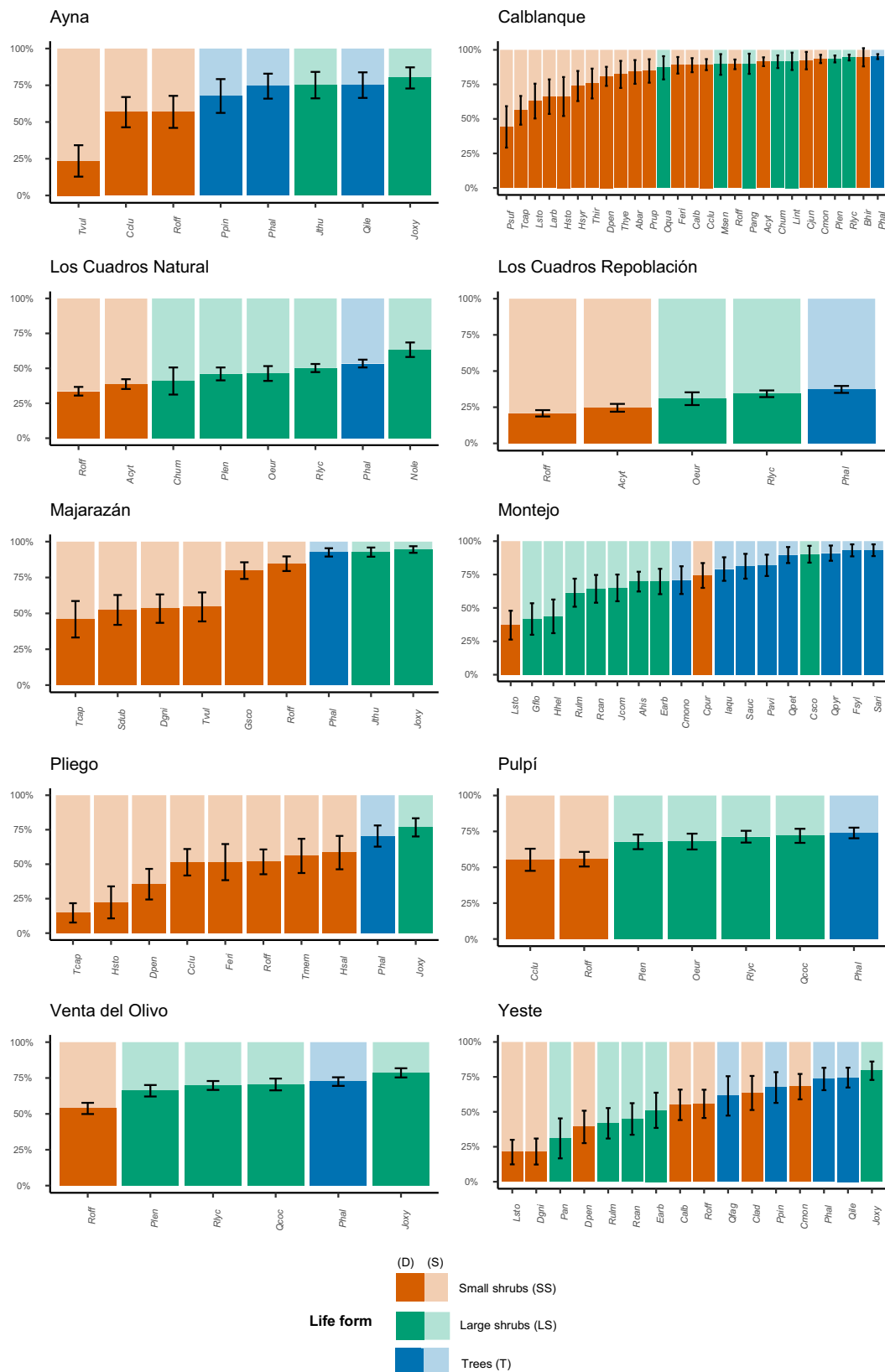


**Fig. 1 | Proportion of shallow vs deep soil water taken up by plants.** Average proportions (%  $\pm$  standard deviation) of shallow (S; 0–20 cm depth; faded colors in upper part of each column) and deep soil water sources (D; >20 cm depth; solid colors in lower part of each column) taken up by coexisting woody plant species at each study site, estimated using Bayesian mixing models (see Material and

Methods section for specific details on calculations).  $N = 6$  individuals per specie in Ayna, Majarazan, Montejo, Pliego, Pulpi and Yeste;  $n = 3$  individuals per specie in Calblanque; and  $n = 10$  individuals per specie in Cuadros Natural, Cuadros Repoblación and Venta Olivo. See Table S2 for species name abbreviations. Source data are provided as a Source Data file.

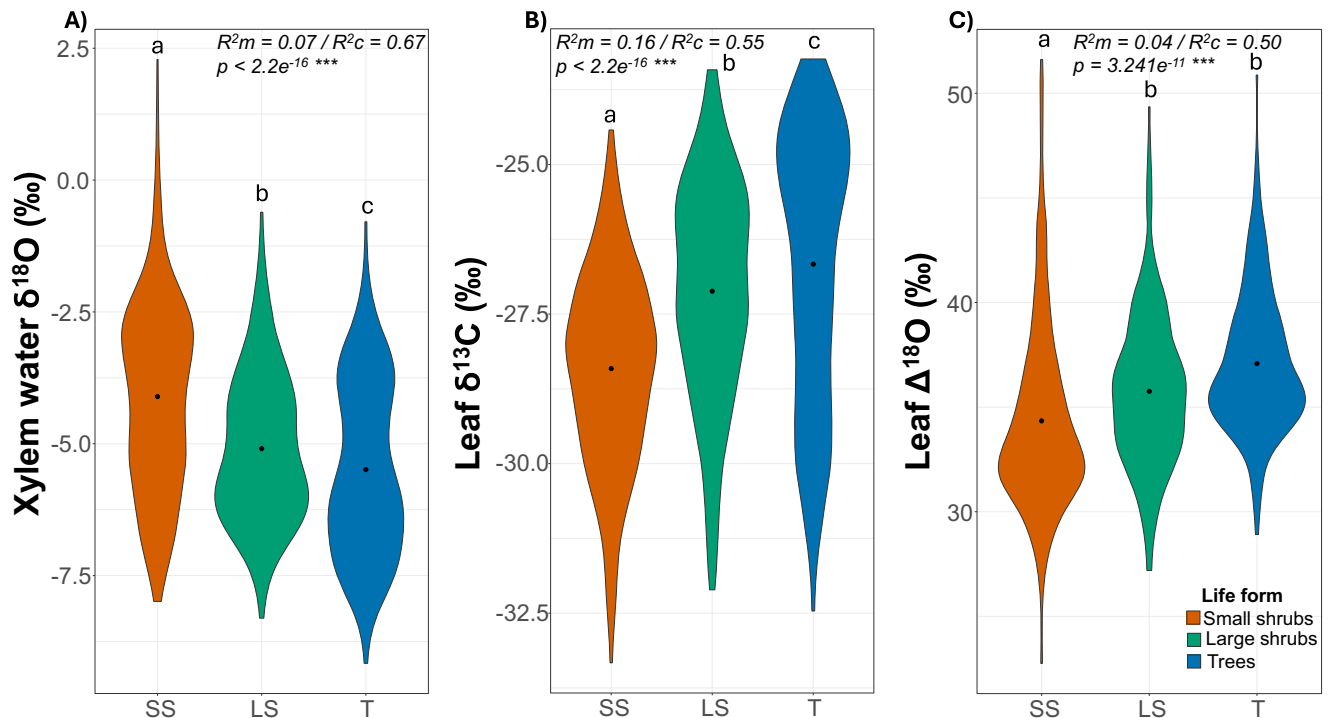


**Fig. 2 | Isotopic differences among plant life forms.** Violin plots depicting xylem water isotopic composition (xylem  $\delta^{18}\text{O}_{\text{XW}}$ ) (A) and leaf isotopic C and O composition (leaf  $\delta^{13}\text{C}_\text{L}$  and  $\Delta^{18}\text{O}_\text{L}$ ; B, C, respectively) by plant life form (small shrubs, large shrubs and trees) across study sites. One-way ANOVA and Tukey's tests were used for multiple comparisons analysis. Black points indicate mean values of each life form. Different letters denote significant ( $p < 0.05$ ) differences

between life forms. Marginal ( $R^2\text{m}$ ) and conditional  $R^2$  ( $R^2\text{c}$ ) indicate the proportion of variance explained by fixed factors or by fixed and random factors in the model, respectively;  $P$  values indicate the significance of each linear mixed model based on F-tests with Satterthwaite approximation of degrees of freedom. Source data are provided as a Source Data file.

tradeoffs between aboveground water use traits ( $\delta^{13}\text{C}_\text{L}$ ,  $\Delta^{18}\text{O}_\text{L}$ , leaf area to sapwood area ratio) and belowground water uptake depth ( $\delta^{18}\text{O}_{\text{XW}}$ ,  $\delta^2\text{H}_{\text{XW}}$ , d-excess<sub>XW</sub>) across coexisting woody plant species and life forms. Our main objective is to address the current knowledge gaps and uncertainty regarding the potential links, interconnectivity and degree of coordination between above- and belowground water use traits across plant species and life forms in Mediterranean ecosystems. More specifically, we aim to identify potential tradeoffs among those traits that might constrain the diversity of whole-plant water use strategies and trait constellations that are ecologically and physiologically feasible and viable for native woody species growing under Mediterranean-type climates. Characterizing the diversity of above and belowground water use traits and their potential coordination and tradeoffs among coexisting plant species at multiple sites with contrasting environmental conditions could provide valuable insights into how native vegetation copes with drought stress in the Mediterranean biome and help improve our current understanding of soil water utilization and partitioning among coexisting individuals in species-rich plant communities<sup>40,41</sup>.

Based on the earlier preliminary findings of local-scale studies conducted in Mediterranean-type ecosystems<sup>5,18,23,25</sup> we hypothesize that: (i) Coexisting woody species and plant life forms exhibit distinct ecohydrological niche segregation driven by size-related differences in soil water uptake depth ( $\delta^{18}\text{O}_{\text{XW}}$ ,  $\delta^2\text{H}_{\text{XW}}$ , d-excess<sub>XW</sub>) between shallow- and deep-rooted species (H1); (ii) Coexisting species and plant life forms also exhibit large differences in leaf-level stomatal regulation stringency and water use efficiency ( $\delta^{13}\text{C}_\text{L}$ ,  $\Delta^{18}\text{O}_\text{L}$ ) ranging from profligate water-spender to conservative water-saving strategies at leaf level (H2); (iii) Aboveground hydraulic traits are coordinated across species and plant functional types, so that a more profligate water-use strategy at leaf level (lower  $\delta^{13}\text{C}_\text{L}$ ,  $\Delta^{18}\text{O}_\text{L}$ ) will be compensated by a lower

leaf area to sapwood area ratio<sup>42</sup> (H3); (iv) Aboveground water use traits ( $\delta^{13}\text{C}_\text{L}$ ,  $\Delta^{18}\text{O}_\text{L}$ , leaf area to sapwood area ratio) are also coordinated with belowground water uptake depth ( $\delta^{18}\text{O}_{\text{XW}}$ ,  $\delta^2\text{H}_{\text{XW}}$ , d-excess) across coexisting woody species and life forms, with water-spenders exhibiting a shallower rooting depth and water uptake pattern than water-saver species (H4); (v) The diversity of whole-plant water use strategies present in upland Mediterranean ecosystems is limited and constrained by the tight coordination and tradeoffs between above- ( $\delta^{13}\text{C}_\text{L}$ ,  $\Delta^{18}\text{O}_\text{L}$ , leaf area to sapwood area ratio) and belowground ( $\delta^{18}\text{O}_{\text{XW}}$ ,  $\delta^2\text{H}_{\text{XW}}$ , d-excess) water use traits (H5); (vi) Interspecific differences in above- and belowground water use traits among coexisting woody species (water uptake depth, leaf  $\delta^{13}\text{C}_\text{L}$ ,  $\Delta^{18}\text{O}_\text{L}$ ) remain largely stable through time, so that within-site isotopic trait-based species rankings are well preserved between dry and wet years (H6).

Here, we show that water source partitioning and ecohydrological niche segregation driven by differences in water uptake depth among coexisting species are widespread across Mediterranean plant communities with contrasting climatic conditions. Foliar carbon and oxygen isotopes indicate that leaf-level stomatal regulation stringency and water-use efficiency also differ greatly among coexisting species and are both tightly coordinated with water uptake depth. Larger and taller trees generally use a greater proportion of deeper soil water, display more conservative water use traits at leaf level (“water-savers”) and show greater investment in foliage relative to shoots. Conversely, smaller shrubs rely mainly on shallow soil water, exhibit a more profligate water use strategy at leaf level (“water-spenders”) and invest more heavily in shoots relative to foliage. Drought and heat stress appear to favor coordination between above and belowground water-use traits, resulting in possibly unavoidable tradeoffs that constrain the diversity of whole-plant water use strategies in Mediterranean plant communities.

## Results

### Vertical soil water source segregation and partitioning among coexisting woody species is widespread in Mediterranean plant communities

At the peak of the Spring growing season, soil water content increased steeply with soil depth at all the study sites except for the wettest location (Montejo; Fig. S1A). We encountered marked soil water isotopic gradients with depth along the soil profile at all the study sites; topsoil water  $\delta^{18}\text{O}$  and  $\delta^2\text{H}$  values were always isotopically enriched relative to rainwater, and soil water isotopic values became progressively more depleted (i.e. more negative) with increasing depth along the edaphic profile (Fig. S1B, C). As a result, soil water d-excess values were always more negative near the surface (indicating intense evaporative isotopic fractionation) and became less negative with increasing soil depth at all the study sites (Fig. S1D). Soil water isotopic  $\delta^{18}\text{O}$  and  $\delta^2\text{H}$  depletion curves generally saturated at 20 cm depth at all the sites (except at the wettest site Montejo, where they saturated at 15 cm), below which soil water isotopic composition remained rather stable throughout the soil profile (Fig. S1). Water stored in deeper soil layers generally showed an isotopic composition that was very close to the Local Meteoric Water Line (LWML) for the Iberian Peninsula at all the sites (Fig. S2A), revealing small or negligible evaporative isotopic enrichment of water stored below 20 cm depth during Spring.

We found evidence of distinct ecohydrological niche segregation and vertical water source partitioning among coexisting woody species at every study site, thereby supporting hypothesis 1 (H1). All the target plant species used varying mixtures of both isotopically enriched topsoil water and deeper, more depleted water sources closer to the Iberian Water Meteoric Line (Fig. S2B). Moreover, a clear water uptake depth continuum ranging from species using predominantly shallow soil water sources to species using mostly deep-water pools was encountered at all the study sites, evidencing a wide variety of coexisting water use strategies leading to distinct ecohydrological niche segregation within Mediterranean plant communities (Fig. 1). We encountered a wide range of soil water uptake patterns among woody plant species, ranging from the small, drought semideciduous shrub *Teucrium capitatum* (Teu cap) that used 85.7 % of shallow topsoil water (<20 cm) at the Pliego site, to the winter-deciduous tree *Sorbus aria* using only 6.4 % of shallow topsoil water at the Montejo site (Fig. 1). Within each study site, plant size (height) strongly influences the proportion of shallow soil water used by each woody species (Fig. S3A, B). Smaller shrubs exhibit much heavier reliance on the topsoil water pool (i.e. higher  $\delta^{18}\text{O}_{\text{sw}}$  values) than neighboring larger shrubs or trees within the same plant community (Fig. 2A) at all the sites. Conversely, small shrub species consistently use a smaller proportion of deep-water sources than larger shrub species at all sites, with taller tree species using the largest proportion of water stored in deep soil/bedrock layers ( $50.3 \pm 0.05\%$ ,  $64.2 \pm 0.05\%$  and  $75.5 \pm 0.06\%$ , respectively, Fig. S4). Moreover, evergreen species used a greater proportion of water stored in deep soil/bedrock layers (lower  $\delta^{18}\text{O}_{\text{sw}}$  values) than coexisting drought-deciduous or semideciduous species across sites (Fig. S5A). We encountered a tight coordination between species maximum rooting depth (obtained from the scientific literature) and water extraction depth ( $\delta^{18}\text{O}_{\text{sw}}$ ), with deeper-rooted species consistently using a greater proportion of deep water sources (more negative  $\delta^{18}\text{O}_{\text{sw}}$ ) (Fig. S6).

### Coordination between belowground water uptake depth and aboveground leaf-level water use traits: the role of phylogeny

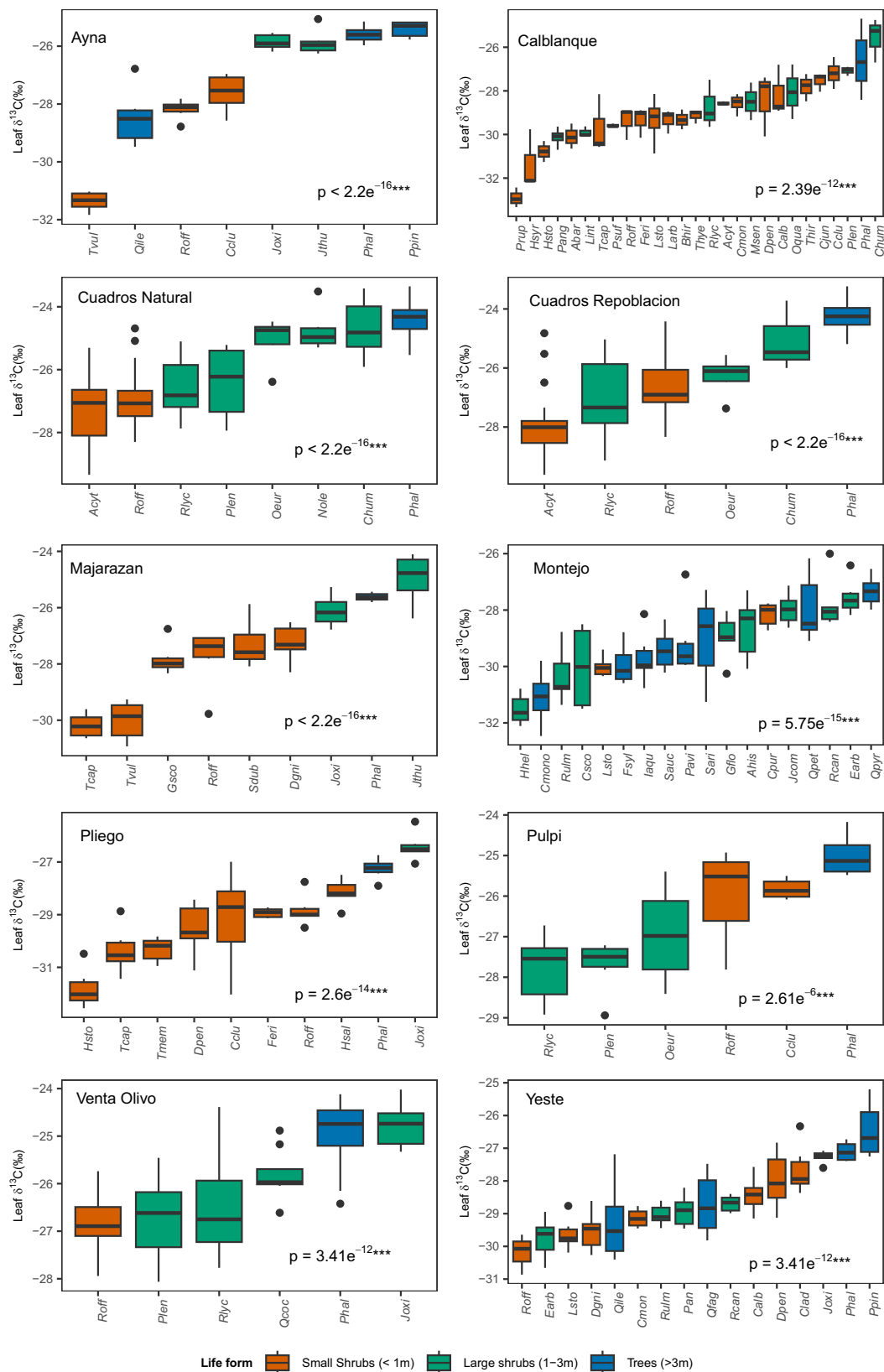
We encountered a remarkably wide range of variation in mean  $\delta^{13}\text{C}_\text{L}$  values among coexisting woody species at every study site, with interspecific variation ( $|\delta^{13}\text{C}_\text{L} \text{ max} - \delta^{13}\text{C}_\text{L} \text{ min}|$ ) within sites ranging between 2.1 and 7.3‰ (Fig. 3). Our findings demonstrate that large interspecific differences in leaf-level intrinsic water use efficiency among coexisting woody species are widespread in Mediterranean

ecosystems, regardless of the contrasting climates among study sites, thereby supporting H2. Within-site variation in mean leaf  $\Delta^{18}\text{O}_\text{L}$  values among coexisting woody species ( $|\Delta^{18}\text{O}_\text{L} \text{ max} - \Delta^{18}\text{O}_\text{L} \text{ min}|$ ) was even larger, ranging between 3.1 and 14.7‰ (Fig. S7). Moreover, we found a strong positive relationship between leaf  $\Delta^{18}\text{O}_\text{L}$  and  $\delta^{13}\text{C}_\text{L}$  values across coexisting woody species (Fig. 4A, B) for both the 2019 and 2022 datasets, which we interpret as evidence that species with tighter stomatal regulation of plant water flux (higher  $\Delta^{18}\text{O}_\text{L}$ ) generally achieve higher intrinsic water use efficiency within each site (higher  $\delta^{13}\text{C}_\text{L}$ ). Both  $\Delta^{18}\text{O}_\text{L}$  and  $\delta^{13}\text{C}_\text{L}$  showed a strong phylogenetic signal (Pagel's  $\lambda = 0.56$ ,  $p < 0.001$  and Pagel's  $\lambda = 0.55$ ,  $p < 0.01$ , respectively). However, the positive relationship between  $\Delta^{18}\text{O}_\text{L}$  and  $\delta^{13}\text{C}_\text{L}$  held robust and remained significant when phylogeny was explicitly considered in the model for both study years ( $z = 2.145$ ,  $p < 0.05$  in 2019;  $z = 3.274$ ,  $p < 0.01$  in 2022).

Principal component analysis (PCA) based on plant height and isotopic water use traits of all 62 woody species across sites revealed a tight coordination among multiple above- and belowground traits, lending support for H4 and H5. For most of these traits, species explained a larger proportion of variance than site, excepting  $\delta^{18}\text{O}_{\text{sw}}$  for which site absorbed a higher proportion of variance. (due to geographically driven variation in rainwater  $\delta^{18}\text{O}$ ; Fig. S8). The first two PCA axes explained 63.6% of the total trait variability across species and sites. The first axis explained 32.8% of the plant trait variation, with height,  $\delta^{18}\text{O}_{\text{sw}}$  and  $\delta^{13}\text{C}_\text{L}$  contributing substantially to this axis (Table S3). Plant life forms absorbed most of the variance along axis 1 (Table S4), as tree species showed larger size, higher  $\delta^{13}\text{C}_\text{L}$  indicating higher water use efficiency and lower  $\delta^{18}\text{O}_{\text{sw}}$  indicating a deeper water extraction pattern, while small shrub species exhibited opposite traits (Fig. 5A). The second axis of the PCA explained 30.8% of total trait variation, largely reflecting differences in environmental conditions among study sites, as site absorbed the largest proportion of variance along this axis (Table S4). Cooler and wetter sites like Montejo or Yeste plot on the positive side of the second PCA axis, whereas warmer and drier sites like Pulpi or Los Cuadros plot on the negative side of this axis (Fig. 5B). However, one of the warmest and driest sites, Calblanque, showed positive scores in the second PCA axis, likely due to its constant exposure to humid marine winds, given that this coastal site is located very near the Mediterranean shore (200–300 m distance only).

The large within-site variation in  $\delta^{13}\text{C}_\text{L}$  and  $\Delta^{18}\text{O}_\text{L}$  among coexisting woody species is strongly modulated by plant size (Fig. S3 C, D) and life form, as smaller shrubs generally show lower  $\delta^{13}\text{C}_\text{L}$  and  $\Delta^{18}\text{O}_\text{L}$  values (lower time-integrated WUEi driven by looser stomatal regulation of plant water flux) than coexisting larger shrubs or trees at all the sites (Fig. 2B, C). The strong within-site negative relationships observed between  $\delta^{13}\text{C}_\text{L}$  and  $\delta^{18}\text{O}_{\text{sw}}$  across coexisting species for both the 2019 and 2022 datasets revealed lower leaf-level intrinsic water use efficiency in smaller-sized species with shallower soil water uptake depth (Fig. 4C, D). This interpretation was further supported by the strong positive relationships found between leaf  $\Delta^{18}\text{O}_\text{L}$  and d-excess<sub>sw</sub>, which indicates looser stomatal regulation of plant water flux in smaller-sized species with a shallower water uptake pattern (Fig. 4 E,F). Deuterium-excess<sub>sw</sub> did not show phylogenetic signal (Pagel's  $\lambda = 6.64 \cdot 10^{-5}$ ,  $p = 1.0$ ) although  $\delta^{18}\text{O}_{\text{sw}}$  did (Pagel's  $\lambda = 0.49$ ,  $p < 0.05$ ). The strong relationship between foliar  $\Delta^{18}\text{O}_\text{L}$  and d-excess<sub>sw</sub> across coexisting woody species was very robust and was not modified when phylogenetic effects were considered ( $z = 6.819$ ,  $p < 0.001$  in 2019;  $z = 8.931$ ,  $p < 0.001$  in 2022). In contrast, the negative relationship between leaf  $\delta^{13}\text{C}_\text{L}$  and  $\delta^{18}\text{O}_{\text{sw}}$  appears to be driven mainly by phylogenetic effects in both study years as these relationships become non-significant when phylogenetic effects are included ( $z = 0.242$ ,  $p = 0.808$  in 2019;  $z = 0.002$ ,  $p = 0.99$  in 2022). Leaf habit also had a strong influence on  $\delta^{13}\text{C}_\text{L}$  and  $\Delta^{18}\text{O}_\text{L}$  variation among coexisting woody species, as drought-deciduous or





semideciduous species showed significantly lower  $\delta^{13}\text{C}_\text{L}$  and  $\Delta^{18}\text{O}_\text{L}$  values than their coexisting evergreen species (Fig. S5B, C).

Mixed models revealed a positive relationship between species height and the leaf: sapwood area ratio, indicating a larger transpiring foliage area per unit cross-sectional sapwood area supplying water to leaves (i.e. lower Huber values) in larger and taller species (Fig. 6A).

Small shrub species exhibited lower leaf: sapwood area ratios (i.e. higher Huber values) than their coexisting large shrub and tree species, while the latter did not differ from each other (Fig. S9). Mixed models also revealed a strong negative correlation between leaf: sapwood area ratio and  $\delta^{18}\text{O}_{\text{LW}}$  across coexisting species (Fig. 6B) that was maintained when accounting for phylogenetic effects ( $z = 4.824$ ;  $p < 0.001$ ), which

**Fig. 3 | Differences in leaf  $\delta^{13}\text{C}$  among coexisting plant species.** Variation of mean leaf carbon isotopic composition ( $\delta^{13}\text{C}_\text{L}$ ) among coexisting woody plant species growing at 10 contrasting study sites. Boxplots represent median (line) species values for  $\delta^{13}\text{C}_\text{L}$  from linear models within each site. Lower and upper hinges correspond to the 25th and 75th percentiles and whiskers depicts 1.5 $\times$ IRQ (interquartile ranges); outlier values are also shown. *P* values depict significant differences between species based on F-test analysis. Different colors depict different plant life

forms. Interspecific variation in average  $\delta^{13}\text{C}_\text{L}$  values among coexisting species was remarkably large within sites (e.g.  $-25.6$  to  $-32.9\text{‰}$ , in Calblanque), often encompassing much of the full range of  $\delta^{13}\text{C}_\text{L}$  values observed at global scale in C3 plants ( $-20$  to  $-33\text{‰}$ )<sup>108</sup>.  $N = 6$  individuals per species in Ayna, Majarazan, Montejo, Pliego, Pulpi and Yeste;  $n = 3$  individuals per species in Calblanque; and  $n = 10$  individuals per species in Cuadros Natural, Cuadros Repoblacion and Venta Olivo. See Table S2 for species name abbreviations. Source data are provided as a Source Data file.

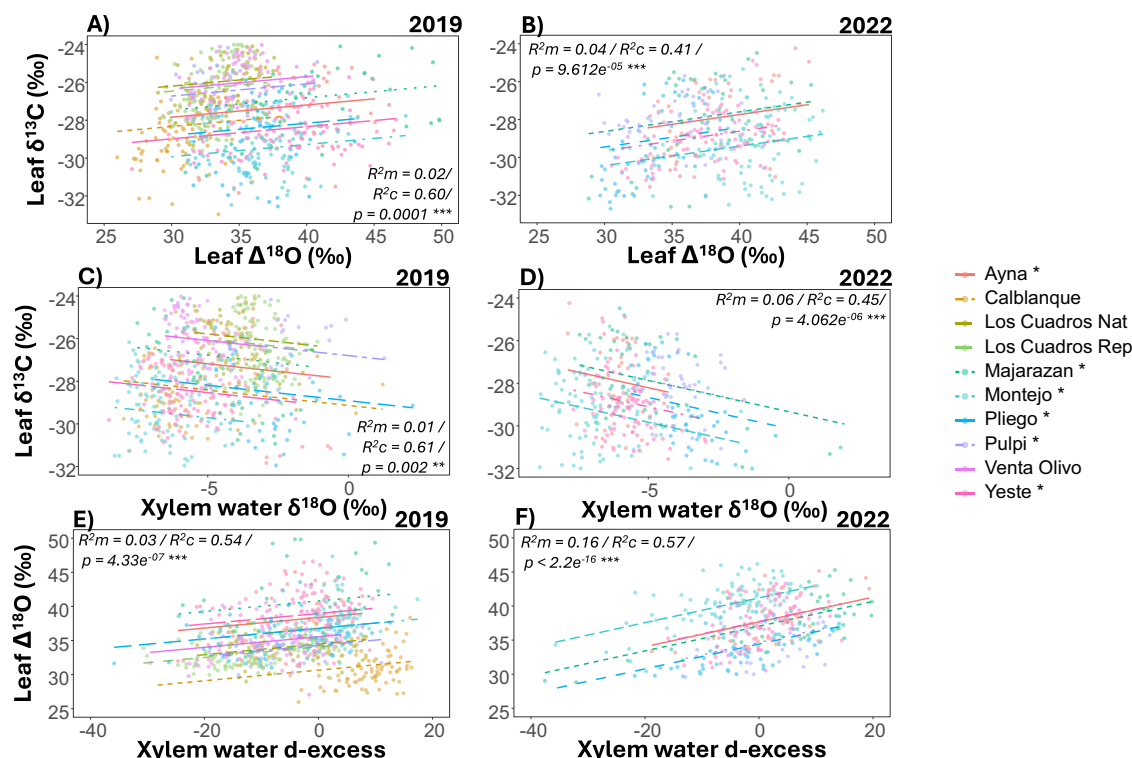


**Fig. 4 | Relationships between leaf isotopes and xylem water isotopes.** Within-site relationships between leaf carbon isotopic composition ( $\delta^{13}\text{C}_\text{L}$ ) and leaf oxygen isotopic composition ( $\Delta^{18}\text{O}_\text{L}$ ; **A, B**); between leaf  $\delta^{13}\text{C}_\text{L}$  and xylem water oxygen isotopic composition ( $\delta^{18}\text{O}_\text{xw}$ ; **C, D**); and between leaf  $\Delta^{18}\text{O}_\text{L}$  and deuterium-excess in xylem water (d-excess<sub>xw</sub>; **E, F**) across individuals of coexisting woody plant species in two different years (2019 and 2022) at multiple sites. Regression lines per site from linear mixed regression models are shown. Colored dots represent

individual plants for each site. Marginal ( $R^2\text{m}$ ) and conditional  $R^2$  ( $R^2\text{c}$ ) indicate the proportion of variance explained by fixed factors or by fixed and random factors in the model, respectively; *P* values indicate the significance of each linear mixed model based on F-tests with Satterthwaite approximation of degrees of freedom. Asterisks indicate the six sites that were sampled in both sampling campaigns (2019 and 2022). Source data are provided as a Source Data file.

indicates a smaller foliage area per cross-sectional sapwood area in species with a shallower water uptake pattern. Finally, we also found positive relationships between leaf: sapwood area ratio and both leaf  $\delta^{13}\text{C}_\text{L}$  and  $\Delta^{18}\text{O}_\text{L}$  across coexisting woody species (Fig. 6C, D), indicating that a sparser foliage with smaller transpiring leaf area per sapwood area is linked to looser stomatal regulation and lower time-integrated water use efficiency (thus supporting H3). These relationships were significantly influenced by evolutionary history ( $z = -1.050$ ,  $p = 0.30$ ;  $z = -1.770$ ,  $p = 0.07$ , respectively, when considering phylogenetic effects).

### Isotopic water-use traits provide reliable proxies for species water use strategies in Mediterranean plant communities

In a subset of six study sites, isotopic water-use traits were measured in two years with sharply contrasting rainfall patterns: In 2019 (2021 in Montejo), rainfall amounts during the winter and spring months preceding sampling were below or near the historical average across all sites, whereas in 2022, the winter-spring months were exceptionally wet, with record-breaking rainfall amounts received during March across all the study sites (200–300% or more above the historical average; Fig. S10). As a result, here was a marked offset in leaf isotopic

values between study years, with consistently lower  $\delta^{13}\text{C}_\text{L}$  values in the wet year (2022) relative to the dry year (2019) across species and sites, as shown by a slopes lower than 1 in the mixed models (slope = 0.78, Fig. 7; see also Table S5). This pattern confirmed that most plants were operating at lower water use efficiencies (lower  $\delta^{13}\text{C}_\text{L}$ ) in the wetter year (2022) in response to greater soil water availability and more humid ambient conditions, as expected from physiological theory. This interpretation was further supported by the much lower leaf  $\delta^{18}\text{O}_\text{L}$  values encountered in the exceptionally rainy year of 2022 at all the 5 strictly Mediterranean sites, which indicates greater stomatal aperture with higher stomatal conductance and transpiration rates across species (relative to the previous drier year of 2019; slope = 0.86, Fig. 7; Table S5). Interestingly, the isotope trait-based species rankings within Mediterranean plant communities were remarkably well preserved through time and remained rather concordant between separate years with sharply contrasting climatic conditions at multiple sites (supporting H6). Within-site species rankings in mean  $\delta^{13}\text{C}_\text{L}$  were particularly well preserved between separate years with sharply contrasting rainfall patterns at all the six study sites (Fig. 7A), thereby supporting the view that the mean leaf carbon isotopic composition of each coexisting woody species reflects a species-specific metabolic set-

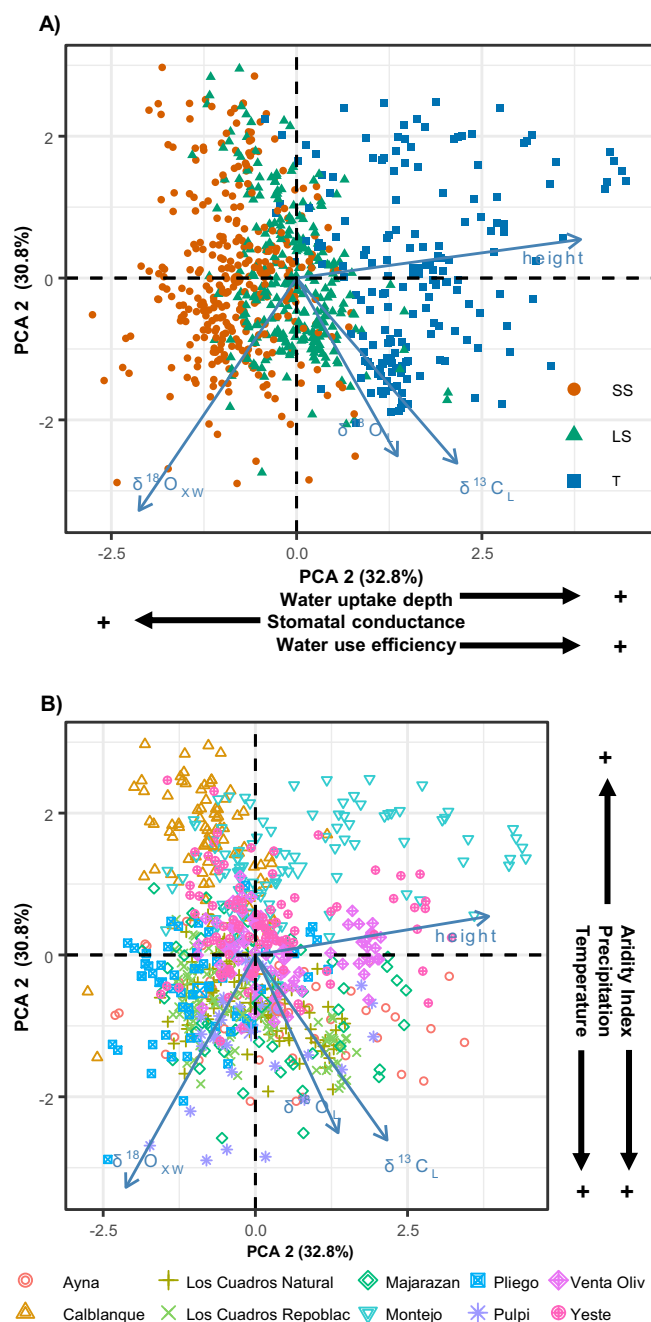


**Fig. 5 | Principal component analysis of key plant traits.** Principal Component Analysis (PCA) of plant leaf isotopic composition ( $\delta^{13}C_L$  and  $\delta^{18}O_L$ ), xylem water oxygen isotopic composition ( $\delta^{18}O_{xw}$ ) and plant height from 63 plant species. Points depict individual plants, colors indicate plant individual plant classification across according to life forms (A) and study site (B). Source data are provided as a Source Data file.

point informing about the trade-off between carbon gain and water loss. Within-site species rankings regarding mean  $\delta^{18}O_{xw}$  (proxy of soil water uptake depth) were also reasonably well preserved between two separate years with sharply contrasting rainfall patterns, indicating that vertical water source partitioning and ecohydrological niche segregation among neighboring woody species during late spring are relatively stable across years at all the study sites (Fig. 7C).

Instantaneous leaf gas exchange measurements in the field revealed that, within each site, smaller shrub species exhibit higher stomatal conductance and transpiration rates and thus operate at lower water use efficiency than neighboring tree or large shrub species

(Fig. S11). Furthermore, we found a significant positive correlation between mean species  $\delta^{13}C_L$  and  $WUE_i$  across coexisting woody species within sites (Fig. 8A), which is remarkable considering the very different timescales involved in both measurement types (time-integrated over several months for carbon isotopes versus snapshot instantaneous measurements for IRGA-based  $WUE_i$ ). This finding confirmed that, within each plant community, a higher species mean  $\delta^{13}C_L$  value is indeed linked to higher intrinsic water use efficiency, as expected from stable isotope theory. Analogous to the strong relationship encountered between  $\delta^{13}C_L$  and  $\Delta^{18}O_L$  across coexisting species within sites, we found a strong within-site association between IRGA-measured  $WUE_i$  and  $g_s$  that further indicates that species exhibiting lower stomatal conductance can achieve higher intrinsic water use efficiency at leaf level (Fig. 7B). A significant negative correlation was also found between  $\Delta^{18}O_L$  and IRGA-measured  $g_s$ , as expected from stable isotope theory (Fig. S12).

## Discussion

Our study demonstrates that distinct vertical ecohydrological niche segregation driven by differences in soil water uptake depth among coexisting woody species is widespread and ubiquitous during the peak of the growing season across Mediterranean plant communities with contrasting climates (Fig. 1, H1). Smaller shrub species are heavily dependent on shallow water sources present in the topsoil layer (0–20 cm) at all sites, while larger woody species (large shrubs and trees) use a greater proportion of deeper (>20 cm) soil water sources that are more reliable and stable through time (Fig. S4). The shallow and deep soil water pools differ markedly in their exposure to direct evaporative loss, their stability and reliability through time, their accessibility to plant roots, and in the contrasting intensity of inter-plant competition for each resource pool<sup>43–45</sup>. Distinct vertical water niche segregation among coexisting woody species should enhance the drought resistance, resilience and overall productivity of diverse plant communities through complementarity effects, a more exhaustive utilization of the most limiting resource along the full soil/bedrock profile, and the attenuation of interspecific competition for soil water<sup>46,47</sup>. Several local-scale studies have reported that moisture stored deep in the soil/bedrock profile is mainly recharged by winter precipitation and represents an important water source for many evergreen and winter-deciduous tree species during the subsequent growing season in Mediterranean-type ecosystems and elsewhere<sup>48–51</sup>. It is noteworthy that we found marked ecohydrological niche segregation among coexisting woody species during the Spring growing season when soil water availability and climatic conditions are relatively favorable, and vegetation is most physiologically active at all the study sites (Fig. 1). Vertical niche segregation in soil water uptake depth among coexisting species would be expected to become even more pronounced during the summer hot drought period, as deep-rooted species progressively shift to deeper water uptake due to topsoil desiccation<sup>25,52,53</sup>.

As noted by several recent studies, the considerable hydraulic pathway length for internal water transport in large trees can lead to substantial time delays between soil water uptake by roots and the isotopic signature of this xylem sap reaching the canopy branches sampled for isotope measurement<sup>54–57</sup>. This so-called “height effect” may complicate the interpretation of the xylem water isotopic composition encountered in upper canopy branches, thereby compromising the correct identification of the soil water sources that tall trees are using at any given time<sup>58–62</sup>. However, the occurrence of long time lags between soil water uptake by roots and internal water transport to the sites of stem sampling in trees seems very unlikely in our study, for the following reasons. First, the average height of the trees sampled in our study was only 8.5 m (ranging from 3 to 20 m height), which significantly limits the length of the hydraulic pathway and travel time for water transport from roots to the sites of sampling (sun-exposed mid



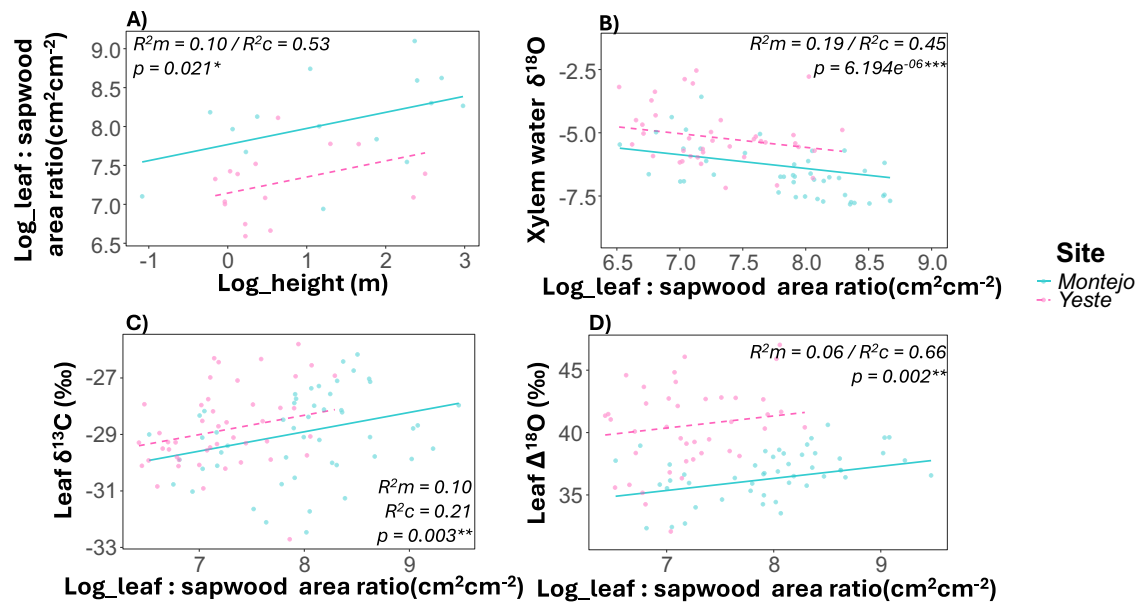


**Fig. 6 | Relationships of leaf area: sapwood area ratio with other key plant traits.** Within-site relationships between leaf area to cross-sectional sapwood area (cm² m⁻²) of terminal shoots and plant height (A), xylem water  $\delta^{18}O_{xw}$  (B), leaf  $\delta^{13}C_L$  (C) and  $\Delta^{18}O_L$  (D) for individual plants from the Montejo and Yeste sites (N = 151 individuals of 29 species). Models are linear mixed regression models with site as random effect. Colored dots represent individual plants at each site except for (A)

where mean values per species were shown. Marginal ( $R^2m$ ) and conditional  $R^2$  ( $R^2c$ ) indicate the proportion of variance explained by fixed factors or by fixed and random factors in the model, respectively; P values indicate the significance of each linear mixed model based on F-tests with Satterthwaite approximation of degrees of freedom. Source data are provided as a Source Data file.

canopy branches). Second, the high xylem sap velocity typically encountered in native trees during the spring growing season under Mediterranean conditions (characterized by high ambient temperature and VPD) favors rapid internal water transport and travel times in trees, thereby leading to relatively short or negligible time lags between root water uptake and transport to the mid canopy branches sampled in our study. For example, Cohen et al.<sup>63</sup> reported that xylem sap velocity, measured with the heat-pulse method, reached 22–68 cm per hour in Aleppo pine (*Pinus halepensis*) and 33–108 cm per hour in holm oak trees (*Quercus ilex ssp. rotundifolia*) growing under semiarid or dry-sub-humid Mediterranean climates in Israel. Such high xylem sap velocities would translate into water travel times from roots to mid canopy branches of 1–2 days or even less in our Aleppo pine and holm oak trees, which were by far the most abundant and widespread tree species across study sites. Seeger and Weiler<sup>64</sup> recently concluded that the potential impacts of hydraulic path length and the so-called “height effect” on tree source water identification can be safely neglected when xylem water transport velocities and canopy transpiration rates are high combined with short transport distances between roots and the sites of sampling, as was always the case in our own study. Moreover, distinct ecohydrological niche segregation between trees and co-occurring small shrubs was strongly supported in our study by the highly significant correlation encountered between the maximum rooting depth of the different species and their xylem water isotopic composition across all plant life forms (Fig. S8).

Overall, our findings support our assumption that leaf carbon and oxygen isotopes provide valuable time-integrative proxies for interspecific variations in intrinsic water use efficiency and stomatal conductance among coexisting woody species, and thus can be considered as useful integrative physiological traits, at least for water-limited Mediterranean plant communities<sup>5,18,23</sup>. We found that the belowground water uptake depth pattern of each species has a marked influence on its aboveground isotopic traits involved in leaf-level water use and flux regulation<sup>65,66</sup>. Within each study site, leaf-level stomatal regulation stringency and intrinsic water use efficiency vary widely (H2) and are both coordinated with soil water uptake depth across

coexisting woody plant species (Fig. 4; H4). Larger and taller woody species, mostly of evergreen leaf habit (and some winter deciduous) that use a greater proportion of deeper water sources generally display more conservative water use traits at leaf level (higher  $\Delta^{18}O_L$  and  $\delta^{13}C_L$  in these “water-saver” species). In contrast, smaller shrub species, which are mostly drought-deciduous or semideciduous, rely mainly on shallow soil water sources and exhibit a much more profligate and acquisitive water use strategy at leaf level (lower  $\Delta^{18}O_L$  and  $\delta^{13}C_L$  in these “water-spender” species) within each study site. Water use by small shrub species with a shallow water uptake pattern is thus more tightly coupled to the rapidly fluctuating dynamics of the topsoil water pool than that of neighboring trees or large shrubs with access to deeper and more temporally stable water pools. In this context, the profligate, water-spender strategy (high  $g_s$  and low  $WUE_i$ ) displayed by smaller shrub species with shallow water uptake pattern likely allows them to optimize water capture and use during the narrow windows of opportunity provided by the irregular rainfall events that recharge the topsoil layer in Mediterranean ecosystems. However, this profligate water-spender strategy could lead to rapid soil moisture depletion within their shallow rooting zone and therefore to a faster onset of soil water deficit, drought stress and enhanced risk of drought-induced cavitation and hydraulic failure during subsequent rainless periods<sup>67</sup>. Interestingly, we found that smaller shrubs compensate their high stomatal conductance rates per unit leaf area during wet periods (high  $g_s$ , low  $\Delta^{18}O_L$  and  $\delta^{13}C_L$ ) by reducing their whole-canopy hydraulic demand through lower leaf area to sapwood area ratios (i.e. a smaller transpirative leaf area relative to the cross-sectional sapwood area supplying water to foliage; H3). Small leaves and sparsely foliated shoots and canopy in small shrubs may favor high sapwood water supply rates to foliage, which are needed to sustain high stomatal conductance rates per unit leaf area during favorable periods (Fig. 6). Moreover, small shrub species with predominantly shallow soil water uptake pattern often exhibit a drought-deciduous or semideciduous leaf habit in Mediterranean ecosystems that further reduces total foliage transpirative area during the summer hot drought period (drought-avoider strategy). Our findings are in good agreement with

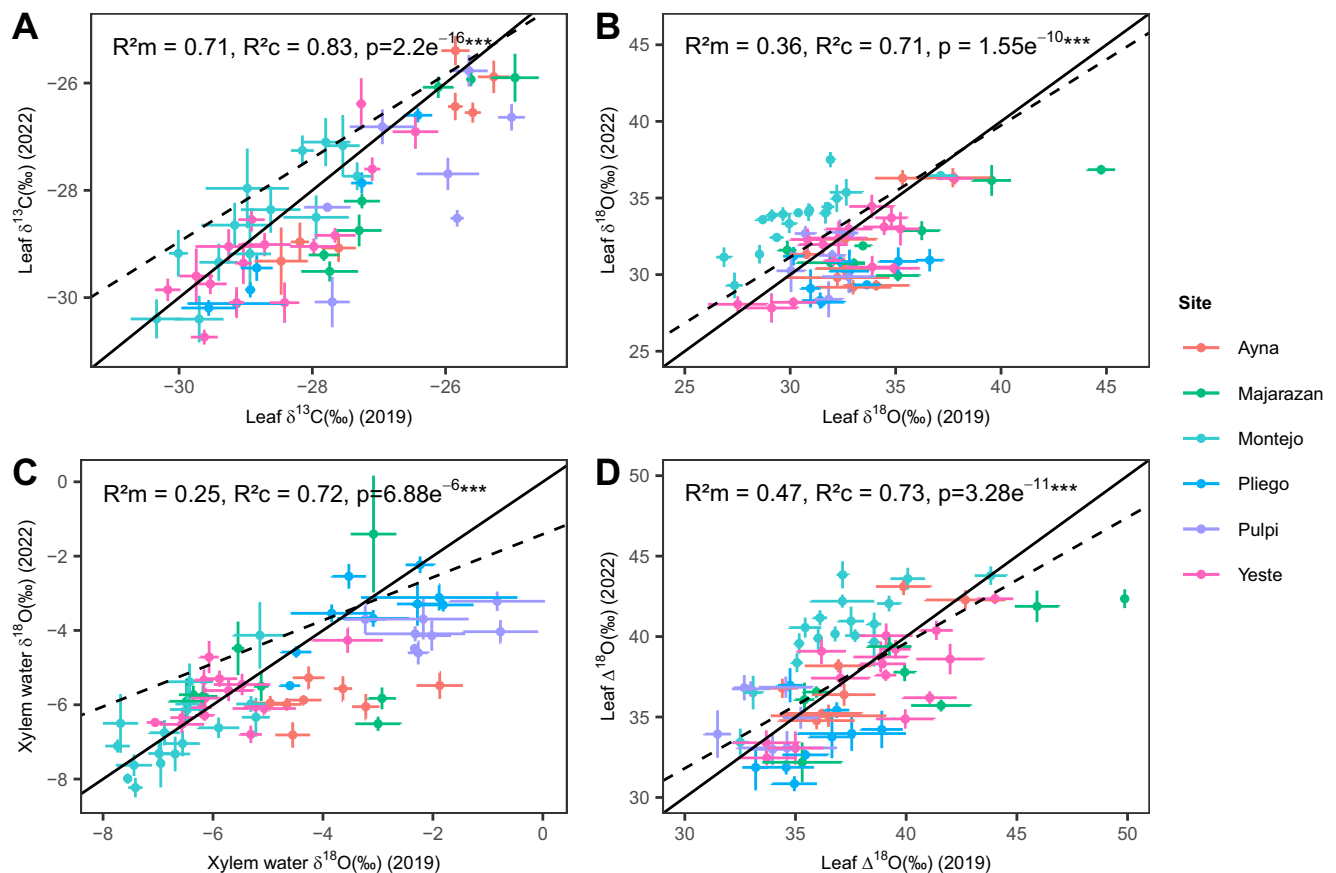


**Fig. 7 | Isotopic rankings among coexisting species are conserved between years with contrasting climatic conditions.** Mean leaf carbon isotopic composition ( $\delta^{13}\text{C}_L$ ) (A), leaf oxygen isotopic composition ( $\delta^{18}\text{O}_L$ ) and calculated as enrichment above source water,  $\Delta^{18}\text{O}_L$  (B and D respectively) and xylem water oxygen isotopic composition ( $\delta^{18}\text{O}_{\text{w}}$ ) (C) for each *species*  $\times$  *site* combination in two separate years with contrasting climatic conditions and rainfall patterns (2019 vs 2022, except for Montejo: 2021 vs 2022).  $N = 6$  individuals per *species*  $\times$  *site* combination in each year. Vertical and horizontal error bars indicate standard errors of

each species mean value in 2019 and 2022 respectively. Solid lines indicate the 1:1 regression line and dashed lines indicate the general regression line from each linear mixed model. Marginal ( $R^2_m$ ) and conditional  $R^2$  ( $R^2_c$ ) indicate the proportion of variance explained by fixed factors or by fixed and random factors in the model, respectively;  $P$  values indicate the significance of each linear mixed based on F-tests with Satterthwaite approximation of degrees of freedom. Source data are provided as a Source Data file.

those of another recent study conducted under semiarid Mediterranean conditions<sup>42</sup>, but differ in part from those of global scale studies that have linked lower leaf area to sapwood area ratio to higher water use efficiency ( $\delta^{13}\text{C}_L$ )<sup>68</sup> and more conservative traits in stems (lower xylem hydraulic conductance)<sup>69</sup>. This disparity could be due to the rather unique constraints that the Mediterranean climate imposes on plants during the prolonged hot and rainless summer drought period, which is the most distinct feature of the Mediterranean biome relative to other dryland ecosystems worldwide.

We found that larger shrub and tree species (mostly evergreen but also including some winter-deciduous trees) in Mediterranean plant communities use a sizeable proportion of deep soil/bedrock water sources even at the peak of the Spring growing season. Deep soil water sources are less easily accessible to roots than topsoil water but are subject to less intense direct evaporative losses and competitive depletion by neighbors, and thus remain more stable over time<sup>70</sup>. Lower  $g_s$  and transpiration rates per unit leaf area and higher time-integrated  $\text{WUE}_i$  with more conservative water use pattern at leaf level (higher  $\Delta^{18}\text{O}_L$  and  $\delta^{13}\text{C}_L$ ) probably allow tall overstory species with deep rooting patterns to sustain a denser and more abundant foliage per sapwood area (higher leaf area: sapwood area ratio, Fig. 6). Furthermore, the emergent canopies of tall overstory woody species are often exposed to harsher and more extreme microclimatic conditions characterized by higher irradiance, temperature, VPD and wind

exposure (compared to the more mesic microclimatic conditions for understorey species of smaller size), which may force trees, especially evergreens (Fig. S4) to adopt more conservative leaf-level water use strategies to withstand these adverse microclimatic conditions<sup>20,71</sup>. Having a tighter stomatal regulation with lower time-integrated stomatal conductance and higher water use efficiency may enable taller tree species to mitigate the drop in xylem water potential in the upper canopy during dry periods associated to their longer hydraulic path-lengths, along with other adaptations in hydraulic architecture and trunk capacitance<sup>20,72</sup>. Interestingly, large evergreen and winter-deciduous species with a predominantly deep water uptake pattern in Mediterranean plant communities are often capable of maintaining growth and physiological activity over longer periods that even extend into the dry summer season (drought-tolerant strategy), and can thus afford a later phenology compared to their neighboring smaller woody species with shallower rooting pattern and drought-deciduous leaf habit<sup>73</sup>.

Interestingly, in our extensive survey of 62 woody plant species across 10 study sites, not every possible combination of above and belowground water use traits was encountered in Mediterranean plant communities. Severe water limitation in upland Mediterranean ecosystems may favor a tight coordination between above and belowground traits<sup>74</sup>, resulting in strong trade-offs among multiple water use traits (Figs. 4 and 6) that may limit the feasibility of certain trait

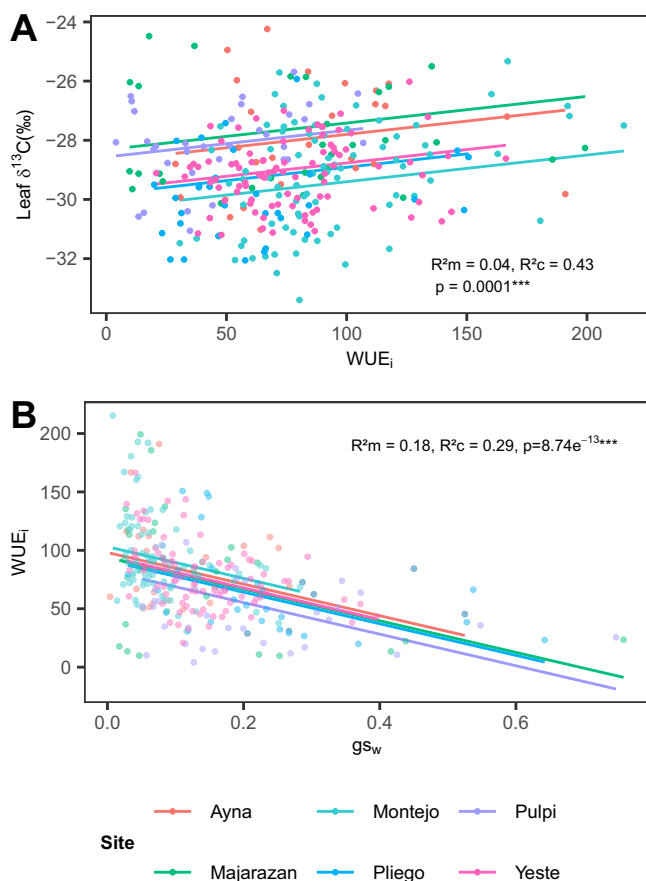


**Fig. 8 | Relationships between leaf  $\delta^{13}\text{C}$ , water use efficiency and stomatal conductance.** Within-site relationships between leaf carbon isotopic composition ( $\delta^{13}\text{C}_L$ ) and instantaneous intrinsic water use efficiency (WUE<sub>i</sub>) measured in the field in the same individuals on the same day in late spring 2022 at each study site (A). Also shown is the relationship between stomatal conductance ( $gs_w$ ) and WUE<sub>i</sub> (B). Regression lines per site obtained from linear mixed regression models are shown. Marginal ( $R^2_{\text{m}}$ ) and conditional  $R^2$  ( $R^2_{\text{c}}$ ) indicate the proportion of variance explained by fixed factors or by fixed and random factors in the model, respectively;  $P$  values indicate the significance of each linear mixed model based on F-tests with Satterthwaite approximation of degrees of freedom. Source data are provided as a Source Data file.

combinations (H5). Interestingly, the combination of a shallow water uptake pattern belowground with a conservative, water-saver leaf-level strategy aboveground was not encountered in any of the target woody species, which suggests that such a combination of water-use traits may not be adaptative or even feasible in Mediterranean dryland environments. In support of this interpretation, a recent study<sup>75</sup> pointed out that acquisitive resource use strategies are preferentially selected over more conservative ones in dryland plant species with short life spans as a way to maximize resource capture and utilization. On the other hand, the combination of a deep-water uptake pattern with a water-spender strategy based on loose stomatal regulation of plant water flux was not encountered in our survey either, as this could also be a maladaptive strategy for large woody plants growing in upland Mediterranean ecosystems. Evergreen or winter deciduous trees deploying a water-spender strategy at leaf level would increase the risk of drought-induced hydraulic failure of long-lived and carbon-costly woody tissues during seasonal summer hot droughts or multi-year droughts when little or no recharge of deep moisture reservoirs takes place<sup>76</sup>. Therefore, the two most widespread and ubiquitous whole-plant water use trait syndromes found in Mediterranean upland ecosystems appear to be either the combination of shallow rooting

pattern with a profligate, water-spender leaf-level strategy (mostly in small drought-deciduous or semideciduous shrubs), or the opposite combination of a deep water uptake pattern with a conservative, water-saver leaf-level strategy (in large evergreen shrubs and evergreen and winter deciduous trees; Fig. 9<sup>8,9</sup>).

Finally, we point out that the tight coordination and strong trade-offs among multiple above- and belowground water use traits encountered in this study may (or may not) be unique and exclusive of the native Mediterranean flora, due to the severe abiotic filters and strong evolutionary pressures imposed by the prolonged hot drought conditions during the summer combined with a winter rainfall pattern. Alternatively, tight coordination and trade-offs among above- and belowground water use traits could be widespread and prevalent across the floras of other water-limited biomes around the world (e.g. drylands with warm-season monsoonal precipitation), even though evolutionary pressures may differ significantly from those operating under a Mediterranean-type climate with a hot dry season<sup>77,78</sup>. This is an intriguing, open question that remains to be elucidated by future work in other drought-prone ecosystems beyond the Mediterranean biome.

## Methods

### Study sites and sampling design

We selected 10 different Mediterranean shrubland, open woodland and closed-canopy forest communities with contrasting climate for the present study (Table S1). These 10 sites were distributed along a 600 km transect from the south-eastern (warmer and drier) to the central part (cooler and wetter) of the Iberian Peninsula. Mean annual precipitation ranged from 272 mm near the Mediterranean coast to 726 mm at the Central Ranges of the Castilian Plateau. Mean annual temperature ranged from 18.5 °C at the coastal sites to 8.6 °C at the Central Ranges site<sup>79</sup>. Mean altitude above sea level of the study sites ranged from 10 m for sites near the Mediterranean coast to 1450 m at the Central Ranges site. Vegetation structure differs dramatically among study sites, from open pine woodlands and shrublands dominated by *Pinus halepensis* and large shrubs (*Rhamnus lycioides*, *Periploca angustifolia*) at the southern and drier coastal sites, to closed-canopy forests dominated by *Pinus pinaster* and *Quercus rotundifolia* in more mesic sites located further inland (e.g. Ayna and Yeste), to multi-layer, closed-canopy forests dominated by *Fagus sylvatica* and *Quercus petraea* in the northernmost and more humid location. Soils are predominantly sedimentary calcareous with a mixture of marls, sandstones and clays depending on the site. Schist formations interspersed with calcareous lithologies can also be found at Calblanque and Montejo<sup>80</sup>.

We collected samples from at least 6 individuals of the most dominant woody species in each plant community, i.e. those overall encompassing 90% of the total cover in the community. In total, we sampled 771 individuals of 62 woody species belonging to 21 plant families, resulting in 121 species-site combinations (Table S6). The species were categorized into three major plant life forms according to their aboveground vegetative height using an adaptation from Raunkaier's life form classification<sup>11,81</sup>: small shrubs (SS, <1 m height), large shrubs (LS, 1–3 m) and trees (T, 3–20 m). Details about the leaf habit (deciduous, evergreen or semideciduous), plant lifespan (long-lived, > 30 years or short-lived, <30 years) and maximum rooting depth were obtained from the scientific literature and our own expert field knowledge for all species<sup>11,82–85</sup> (Table S2). Field sampling campaigns were conducted during the phenological and physiological peak at each location during Spring, starting in early April at the drier and warmer sites (Pulpí, Calblanque, Los Cuadros), continuing in May at sites with typical meso-mediterranean climate (Venta Olivo, Pliego, Ayna, Majarazán, Yeste) and ending in early July at the wettest and coolest site with the latest onset of the growing season (Montejo). The sampling date was carefully chosen at each study site to ensure at least a 2-week period with no rainfall prior to the sampling date. The

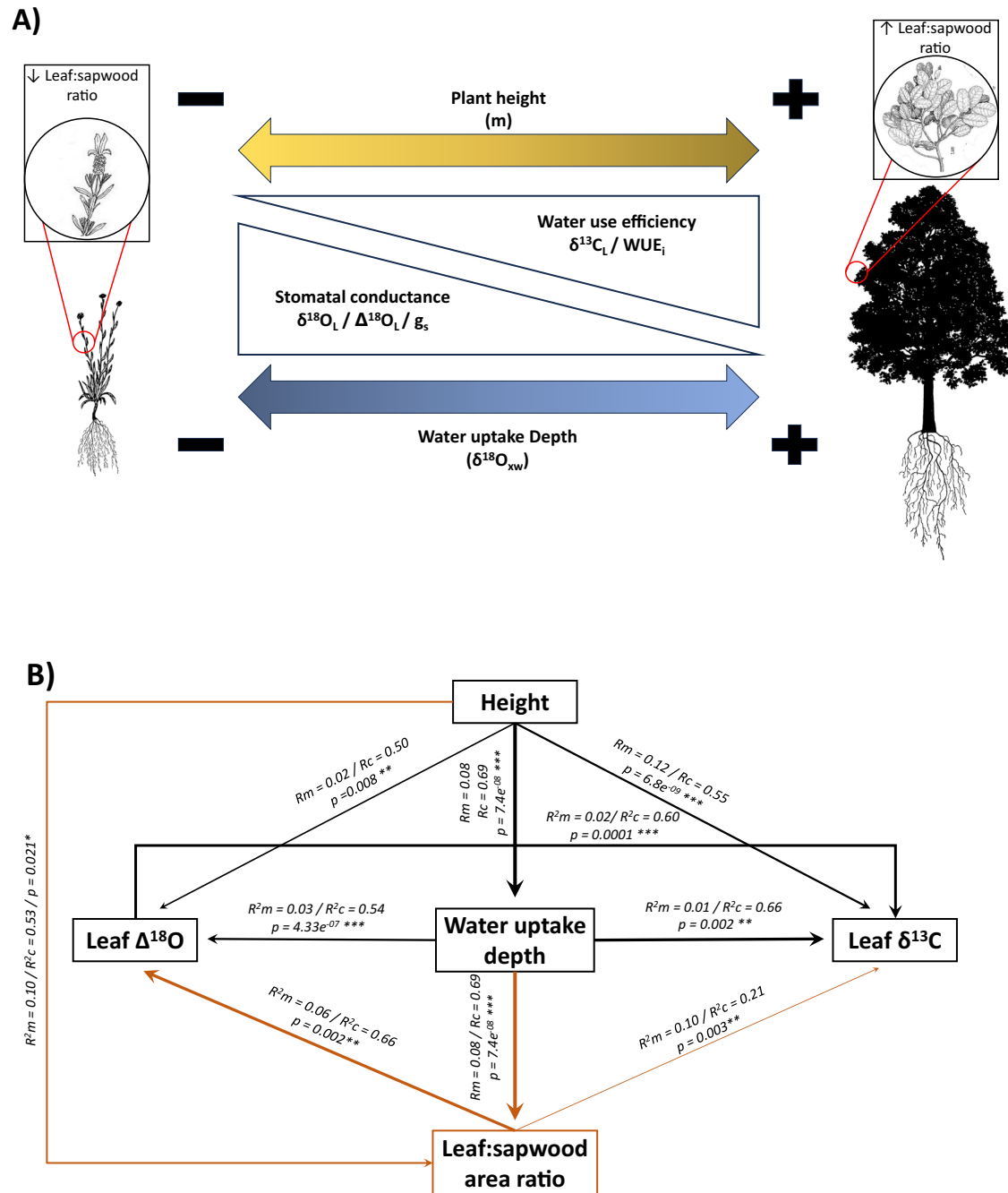


**Fig. 9 | Conceptual model of water-use trait coordination in Mediterranean woody plants. A** Conceptual model summarizing the acquisitive-conservative water-use trait continuum encompassed by coexisting woody plant species in Mediterranean plant communities. At one end of the spectrum, we encounter small-sized species with shallow soil water uptake patterns exhibiting a profligate, water-spender strategy at leaf level (high stomatal conductance and low water use efficiency) and smaller leaf area to sapwood area ratios. At the opposite end of the functional spectrum, we encounter larger-sized species with deeper soil water uptake patterns displaying a more conservative water-saver strategy at leaf level (low stomatal conductance and high water use efficiency) and higher leaf area to sapwood area ratios. Images adapted from Flora Iberica<sup>109</sup>. **B** Correlation network between traits measured in woody species across study sites resulting from performing bivariate linear mixed models with site and life form as crossed random factors. Solid arrows indicate positive relationships between traits, and marginal

and conditional  $r$ -squared values along with the  $p$  values for each model based on  $t$ -test analysis are shown next to arrows. Water uptake depth is based on  $\delta^{18}\text{O}_{\text{xw}}$  data in all models where it is involved, except for its relationship with  $\Delta^{18}\text{O}_\text{L}$ ; in this particular case, for which xylem water deuterium excess has been used instead of  $\delta^{18}\text{O}_{\text{xw}}$  as proxy of water uptake depth, since  $\Delta^{18}\text{O}_\text{L}$  and  $\delta^{18}\text{O}_{\text{xw}}$  are mathematically correlated. Black arrows indicate results from linear mixed models including 10 sites (62 species,  $n = 775$  individuals) and brown arrows indicate results from linear mixed models including only 2 sites (Montejo and Yeste, 33 species,  $n = 151$  individuals). Marginal ( $R^2m$ ) and conditional  $R^2$  ( $R^2c$ ) indicate the proportion of variance explained by fixed factors or by fixed and random factors in the model, respectively;  $P$  values indicate the significance of each linear mixed model based on  $F$ -tests with Satterthwaite approximation of degrees of freedom. Arrows widths are represented according to conditional  $R^2$ -squared values. Source data are provided as a Source Data file.



rationale for this was to ensure the development of a steep soil water isotopic gradient with depth along the edaphic profile, which is typically formed in response to topsoil water evaporation and isotopic fractionation during prolonged rainless periods<sup>28</sup>. Six of the study sites were sampled in two separate years with contrasting climatic conditions and rainfall patterns, as much higher precipitation was recorded in 2022 compared to 2019 (or 2021 in Montejo) across all sites (Fig. S10).

### Xylem and soil water isotopic analyses

For each plant individual, we sampled one basal 5 cm segment of fully lignified stem from a terminal branch, to avoid issues related to potential xylem water isotopic enrichment due to backflow from transpiring leaves or green photosynthetic stems<sup>86</sup>. For tree species, we sampled stem samples from fully sun-exposed mid-canopy branches (at least 3–6 m aboveground level) using a pole-pruner. The stems were debarked to isolate the xylem, stored in 5 ml glass vials, sealed with parafilm to prevent water loss, and stored at  $-20^{\circ}\text{C}$  until water extraction. At each site, we sampled a minimum of 2 and up to 6 soil water profiles, using a cylindrical hand auger with 4 cm diameter (Eijkelkamp, The Netherlands). Soil samples were taken, every 5 cm in the topsoil layer (down to 20 cm) and every 10 cm below 20 cm deep, until we reached impenetrable hard bedrock layers (which were located between 30 and 120 cm deep, depending on soil characteristics at each study site). All freshly collected soil samples were immediately placed in double sealed plastic bags in the field, maintained in a cooler and transported to the laboratory, where a soil subsample was transferred to 5-ml glass vials, sealed with parafilm, and kept at  $-20^{\circ}\text{C}$  until water extraction.

We used a cryogenic vacuum distillation line maintained at  $100^{\circ}\text{C}$  and 10 millitorr vacuum pressure for at least 2 hours to extract all the water contained in plant stems (xylem water) and soil samples<sup>87</sup>. Extracted water samples were shipped to the Center for Stable Isotope Biogeochemistry of the University of California (CSIB-UCB, Berkeley, USA) for isotopic analyses. Water  $\delta^2\text{H}$  composition was determined in a dual inlet using a hot chromium reactor unit (H/Device™; Thermo Scientific, Waltham, MA, USA) interfaced with a Thermo Delta V Plus mass spectrometer (Thermo Fisher Scientific). Continuous flow using a Thermo Gas Bench II interfaced to a Thermo Delta V Plus mass spectrometer was used for analyzing water  $\delta^{18}\text{O}$  composition. Hydrogen ( $\delta^2\text{H}$ ) and oxygen ( $\delta^{18}\text{O}$ ) isotopic composition are expressed in ‰ notation relative to the standard V-SMOW (Vienna standard Mean Ocean Water). Long-term external precision values for water  $\delta^2\text{H}$  and  $\delta^{18}\text{O}$  determinations were  $\pm 0.60\text{‰}$  and  $\pm 0.12\text{‰}$ , respectively. Deuterium excess was calculated as the deviation from the Local Water Meteoric Line (LMLW) for the Iberian Peninsula ( $d\text{-excess} = \delta^2\text{H} - 8.49 \times \delta^{18}\text{O}$ <sup>88</sup>).

### Leaf isotopic and gas exchange measurements

We sampled sun-exposed, fully expanded and healthy-looking leaves from the same branches collected for xylem water extractions in each individual plant. These leaves were immediately placed in sealed bags containing a piece of wet paper in the field, transported to the lab and stored in the fridge at  $4^{\circ}\text{C}$  for leaf material processing within 24–48 h. Leaf samples were oven dried at  $60^{\circ}\text{C}$  for 48 h and finely ground using a ball mill (MM200, Retsh, Germany) before being weighted and encapsulated into tin or silver capsules for leaf  $\delta^{13}\text{C}$  and leaf  $\delta^{18}\text{O}$  isotopic analyses, respectively. Leaf  $\delta^{13}\text{C}$  was measured at CSIB-UCB by continuous flow (CF) dual isotope analysis using a CHNOS Elemental Analyzer interfaced to an IsoPrime100 mass spectrometer, and leaf  $\delta^{18}\text{O}$  was determined in continuous flow (CF) using an Elementar PYRO Cube interfaced to a Thermo Delta V mass spectrometer. Both leaf  $\delta^{13}\text{C}$  and  $\delta^{18}\text{O}$  isotopic composition are expressed in delta notation (‰) relative to the Vienna Pee Dee Belemnite standard (V-PDB) and the Vienna Standard Mean Ocean Water (VSMOW), respectively. Long-term external precision values for leaf  $\delta^{13}\text{C}$  and  $\delta^{18}\text{O}$  determinations

were  $\pm 0.10\text{‰}$  and  $\pm 0.20\text{‰}$ , respectively. As a way to isolate the leaf-level evaporative signal from the source water isotopic signal<sup>32</sup>, we calculated the oxygen isotopic enrichment of leaf organic matter above the isotopic composition of plant source water, as the difference between the  $\delta^{18}\text{O}$  value of bulk leaf material and the  $\delta^{18}\text{O}$  value of xylem water in each individual plant:  $\Delta^{18}\text{O}_L = \delta^{18}\text{O}_{\text{leaf}} - \delta^{18}\text{O}_{\text{xylemwater}}$ .

According to stable isotope theory, leaf  $\delta^{13}\text{C}_L$  and  $\Delta^{18}\text{O}_L$  can be considered proxies for time-integrated intrinsic water use efficiency and stomatal conductance, respectively<sup>5,23,30,32,89,90</sup>. To confirm and ensure that this interpretation of leaf C and O isotopic composition as proxies of time-integrated leaf gas exchange was plausible, we also measured photosynthetic rates (A), stomatal conductance ( $g_s$ ) and transpiration rate (E) at the peak of the growing season at 6 of the 10 study sites during the 2022 sampling campaign using a portable infrared gas analyzer (IRGA, LI-6800, LI-COR Inc. Lincoln, NE, USA). We sampled the 40 woody species present in the 6 study areas, measuring 6 individuals of each species at each site (the same individuals used for isotopic measurements). The LI-6800 equipment had a  $2\text{ cm}^2$  leaf cuvette and a  $\text{CO}_2$  injector. Leaf gas exchange was measured on fully sun-exposed leaves between 9:00 and 13:00 a.m. (GMT) and expressed on a total leaf surface area basis. All leaf gas exchange measurements were made at saturating light intensity of  $1500\ \mu\text{mol mol}^{-2}\text{ s}^{-1}$  and at ambient air temperature and air humidity, with the air flux set to  $350\ \mu\text{mol s}^{-1}$ . The  $\text{CO}_2$  concentration in the cuvette was maintained at  $420\ \mu\text{mol mol}^{-1}\text{ CO}_2$ . Total leaf area was, for some species, smaller than the leaf cuvette ( $2\text{ cm}^2$ ) so we rescaled the measures to the actual leaf area inside the cuvette, which was destructively sampled after IRGA measurements in the field, transported to the lab and measured with a scanner and image software (Photoshop v22.5.0, Tokyo, Japan). Intrinsic water use efficiency ( $\text{WUE}_i$ ) was calculated as the ratio between photosynthetic rate and stomatal conductance ( $A/g_s$ ), whereas instantaneous water use efficiency ( $\text{WUE}_t$ ) was calculated as the ratio between photosynthetic rate and transpiration ( $A/E$ ).

### Plant hydraulic architecture measurements

We measured the leaf area to sapwood area ratio<sup>91</sup> of terminal shoots in three randomly selected individuals of each woody species present at the two most taxonomically diverse and species-rich study sites (Montejo in 2021, 18 sp; Yeste in 2023, 16 sp). A higher leaf area: sapwood area ratio of terminal branches is indicative of higher total transpiring leaf area per unit of cross-sectional sapwood area supplying water to foliage. The total leaf area of terminal branches was carefully measured in the laboratory within 48 h after sampling in the field using a scanner and Adobe Photoshop<sup>92</sup>. Cross-sectional sapwood area was obtained after debarking the distal stem to isolate the xylem and by measuring its diameter with a digital caliper (Storm, Vitoria, Spain). We also measured leaf C and O isotopes and xylem water isotopic composition in these individuals.

### Statistical analysis

To estimate the proportion of shallow vs deep-water sources used by each species at the peak of the Spring growing season, we first set the border between both soil depth interval categories at the depth where the soil water  $\delta^{18}\text{O}$  depletion curve saturated which was between 15 and 30 cm depth depending on the site (Fig. S1). At the Pulpi site, the hardness of the ground and shallow bedrock only allowed us to reach 25 cm deep with the hand auger, and the soil water  $\delta^{18}\text{O}$  depletion curve was not yet saturated at this depth. Soil water isotopic composition data were unavailable for the Venta del Olivo, Los Cuadros Natural and Los Cuadros Repoblacion sites, so we used the average of the top 5% highest individual plant xylem water  $\delta^{18}\text{O}$  values encountered at each site as a proxy for topsoil water  $\delta^{18}\text{O}$  values<sup>28</sup>. At these same 3 sites and Pulpi, where no  $\delta^{18}\text{O}$  data for deep water sources were available, we used the average winter rain isotopic composition as a proxy for the deep water pool, obtained using



geospatial interpolation maps based on GNIP data<sup>93,94</sup>. The isotopic composition of winter precipitation was used as a proxy for the deep water pool since the isotopic composition of water stored in deep soil layers was very similar to that of winter precipitation at the remaining 6 sites (Fig. 1A).

We used Bayesian mixed modelling approach with the MixSIAR package in R<sup>95</sup> to estimate the proportion of deep and shallow soil water used by each woody plant species. We included “site” as a random factor and “species” nested within “site” to account for the variance within a species related to the sites. Given the uncertainties regarding isotopic discrimination against deuterium during water uptake by plant roots<sup>26,27,96</sup> we used only the  $\delta^{18}\text{O}$  of xylem water of each individual for MixSIAR calculations. The mean  $\delta^{18}\text{O} \pm \text{SD}$  of all shallow or deep soil water samples at each site were included as water source data input in the model. We run the model setting manually the number of iterations, burn-in and thinning to 500,000, 200,000 and 300, respectively. Model diagnosis was performed via the Gelman-Rubin and Geweke tests<sup>97</sup>.

This study encompasses 62 woody species belonging to 21 different plant families across 10 sites, so for each trait we assessed the percentage of variance explained by site and species using *calcVarPart* function (package *variancePartition*<sup>98</sup>). Besides, we used Pagel’s Lambda to assess the degree of influence of phylogeny on each trait studied<sup>99</sup>. We ran phylogenetic linear mixed models (PGLMMs)<sup>100</sup> to account for phylogeny effect on correlations among traits, using species phylogeny nested within site. A phylogenetic tree with our target species based on GBOTB, extended phylogeny of vascular plants<sup>101,102</sup> was used as an input in the PGLMMs. We also ran general linear mixed models (GLMMs) without considering the phylogeny, including the site and life form as random crossed effects to account for the differences in climate, continentality, altitude and plant community composition between sites along with differences between plant functional types within each site. We analyzed the influence of plant life form and leaf habit on the leaf and xylem water isotopic composition using GLMM, and then explored the relationships between water uptake depth, leaf water-use traits and maximum rooting depth ( $\Delta^{18}\text{O}_L - \text{leaf } \delta^{13}\text{C}_L$ ,  $\text{leaf } \delta^{13}\text{C}_L - \text{xylem } \delta^{18}\text{O}_{\text{XW}}$  and  $\Delta^{18}\text{O}_L - \text{d-excess}_{\text{XW}}$ ,  $\text{xylem } \delta^{18}\text{O}_{\text{XW}} - \text{root depth}_{\text{max}}$ ) using general mixed regression models. A principal component analysis (PCA) was performed including  $\delta^{13}\text{C}_L$ ,  $\delta^{18}\text{O}_{\text{XW}}$ ,  $\delta^{18}\text{O}_L$  and plant height to obtain a multidimensional overview of the coordination of these key plant traits across sites and life forms. The proportion of the total trait variance explained by plant life form versus site was further evaluated using one-way ANOVAs on the PCA axis 1 and 2 scores of all plant individuals. We also used GLMM to assess the relationships between Leaf area: Sapwood area Ratio and isotopic water use traits ( $\Delta^{18}\text{O}_L$ ,  $\text{leaf } \delta^{13}\text{C}_L$ ,  $\delta^{18}\text{O}_{\text{XW}}$ ) across species, excluding *Cytisus purgans* from the analysis because it has photosynthetic stems with tiny leaves and exhibits an extreme outlier Leaf area: Sapwood area Ratio. We also analyzed the relationship between Leaf area: Sapwood area Ratio and species height, but as we could not measure individual plant height at time of terminal branch sampling, we ran the model using mean Leaf area: Sapwood area Ratios per species and mean species height in Montejo and Yeste, which had been measured in previous field campaigns. To assess the validity of leaf carbon and oxygen isotopes as proxies for intrinsic water use efficiency and stomatal conductance, respectively, we ran general mixed regression models between  $\text{leaf } \delta^{13}\text{C}_L - \text{WUE}_i$ , and  $\text{WUE}_i - g_s$ , while linear regression was run between  $\Delta^{18}\text{O}_L$  and  $g_s$ . All the analyses were conducted with R<sup>103</sup> working with packages *nmle*<sup>104</sup>, *phyr*<sup>105</sup>, *V.phyloMaker*<sup>106</sup> and *MixSIAR*<sup>107</sup>. Trait values mentioned throughout the text are always the mean  $\pm$  standard error (SE).

## Reporting summary

Further information on research design is available in the Nature Portfolio Reporting Summary linked to this article.

## Data availability

The data generated in this study are provided in the Figshare repository with <https://doi.org/10.6084/m9.figshare.27939669> (<https://doi.org/10.6084/m9.figshare.27939669>). Source data are provided with this paper.

## References

- Díaz, S. et al. The global spectrum of plant form and function. *Nature* **529**, 167–171 (2016).
- Bruehlheide, H. et al. Global trait–environment relationships of plant communities. *Nat. Ecol. Evol.* **2**, 1906–1917 (2018).
- Reich, P. B. The world-wide ‘fast-slow’ plant economics spectrum: a traits manifesto. *J. Ecol.* **102**, 275–301 (2014).
- Wright, I. J. et al. The worldwide leaf economics spectrum. *Nature* **428**, 821–827 (2004).
- Moreno-Gutiérrez, C., Dawson, T. E., Nicolás, E. & Querejeta, J. I. Isotopes reveal contrasting water use strategies among coexisting plant species in a mediterranean ecosystem. *N. Phytol.* **196**, 489–496 (2012).
- Araya, Y. N. et al. A fundamental, eco-hydrological basis for niche segregation in plant communities. *N. Phytol.* **189**, 253–258 (2011).
- Silvertown, J., Araya, Y. & Gowing, D. Hydrological niches in terrestrial plant communities: a review. *J. Ecol.* **103**, 93–108 (2015).
- Mooney, H. A. & Dunn, E. L. Photosynthetic system of mediterranean-climate shrubs and trees of California and Chile. *Am. Nat.* **104**, 447–453 (1970).
- Mooney, H. A. & Dunn, E. L. Convergent evolution of Mediterranean-climate evergreen sclerophyll shrubs. *Evolution* **24**, 292–303 (1970).
- Ackerly, D. D. Functional strategies of chaparral shrubs in relation to seasonal water deficit and disturbance. *Ecol. Monogr.* **74**, 25–44 (2004).
- Tumber-Dávila, S. J., Schenk, H. J., Du, E. & Jackson, R. B. Plant sizes and shapes above and belowground and their interactions with climate. *N. Phytol.* **235**, 1032–1056 (2022).
- Laughlin, D. C. et al. Rooting depth and xylem vulnerability are independent woody plant traits jointly selected by aridity, seasonality, and water table depth. *N. Phytol.* **22**, 41 (2023).
- Fan, Y., Miguez-Macho, G., Jobbágy, E. G., Jackson, R. B. & Otero-Casal, C. Hydrologic regulation of plant rooting depth. *Proc. Natl Acad. Sci. USA* **114**, 10572–10577 (2017).
- Sohel, M. S. I., Grau, A. V., McDonnell, J. J. & Herbohn, J. Tropical forest water source patterns revealed by stable isotopes: a preliminary analysis of 46 neighboring species. *For. Ecol. Manage.* **494**, 119355 (2021).
- Evaristo, J. & McDonnell, J. J. Prevalence and magnitude of groundwater use by vegetation: a global stable isotope meta-analysis. *Sci. Rep.* **7**, 1–12 (2017).
- Miguez-Macho, G. & Fan, Y. Spatiotemporal origin of soil water taken up by vegetation. *Nature* **598**, 624–628 (2021).
- Grossiord, C. Having the right neighbors: how tree species diversity modulates drought impacts on forests. *New Phytol.* <https://doi.org/10.1111/nph.15667> (2019).
- Illuminati, A., Querejeta, J. I., Pías, B., Escudero, A. & Matesanz, S. Coordination between water uptake depth and the leaf economic spectrum in a Mediterranean shrubland. *J. Ecol.* **110**, 1844–1856 (2022).
- Bachofen, C. et al. Tree water uptake patterns across the globe. *New Phytol.* <https://doi.org/10.1111/NPH.19762> (2024).
- Fernández-de-Uña, L., Martínez-Vilalta, J., Poyatos, R., Mencuccini, M. & McDowell, N. G. The role of height-driven constraints and compensations on tree vulnerability to drought. *New Phytol.* <https://doi.org/10.1111/nph.19130> (2023).
- Siegwolf, R. et al. The dual C and O isotope – gas exchange model: a concept review for understanding plant responses to the

- environment and its application in tree rings. *Plant Cell Environ.* **46**, 1–22. <https://doi.org/10.1111/pce.14630> (2023).
22. Ding, Y., Nie, Y., Chen, H., Wang, K. & Querejeta, J. I. Water uptake depth is coordinated with leaf water potential, water-use efficiency and drought vulnerability in karst vegetation. *N. Phytol.* **229**, 1339–1353 (2021).
  23. Prieto, I., Querejeta, J. I., Segrestin, J., Volaire, F. & Roumet, C. Leaf carbon and oxygen isotopes are coordinated with the leaf economics spectrum in Mediterranean rangeland species. *Funct. Ecol.* **32**, 612–625 (2018).
  24. Querejeta, J. I., Ren, W. & Prieto, I. Vertical decoupling of soil nutrients and water under climate warming reduces plant cumulative nutrient uptake, water-use efficiency and productivity. *N. Phytol.* **230**, 1378–1393 (2021).
  25. Palacio, S., Montserrat-Martí, G. & Ferrio, J. P. Water use segregation among plants with contrasting root depth and distribution along gypsum hills. *J. Veg. Sci.* **28**, 1107–1117 (2017).
  26. Barbata, A. et al. Evidence for distinct isotopic compositions of sap and tissue water in tree stems: consequences for plant water source identification. *N. Phytol.* **233**, 1121–1132 (2022).
  27. Ellsworth, P. Z. & Williams, D. G. Hydrogen isotope fractionation during water uptake by woody xerophytes. *Plant Soil* **291**, 93–107 (2007).
  28. Allison, G. B., Barnes, C. J. & Hughes, M. W. The distribution of deuterium and  $^{18}\text{O}$  in dry soils 2. *Exp. J. Hydrol.* **64**, 377–397 (1983).
  29. Ehleringer, J. R. & Cerling, T. E. Atmospheric  $\text{CO}_2$  and the ratio of intercellular to ambient  $\text{CO}_2$  concentrations in plants. *Tree Physiol.* **15**, 105–111 (1995).
  30. Dawson, T. E., Mambelli, S., Plamboeck, A. H., Templer, P. H. & Tu, K. P. Stable isotopes in plant ecology. *Annu. Rev. Ecol. Syst.* **33**, 507–559 (2002).
  31. Farquhar, G. D., Ehleringer, J. R. & Hubick, K. T. Carbon isotope discrimination and photosynthesis. *Annu. Rev. Plant Physiol. Plant Mol. Biol.* **40**, 503–537 (1989).
  32. Barbour, M. M. Stable oxygen isotope composition of plant tissue: a review. *Funct. Plant Biol.* **34**, 83–94 (2007).
  33. Farquhar, G. D., Cernusak, L. A. & Barnes, B. Heavy water fractionation during transpiration. *Plant Physiol.* **143**, 11–18 (2007).
  34. Werner, C. & Maguas, C. Carbon isotope discrimination as a tracer of functional traits in a mediterranean macchia plant community. *Funct. Plant Biol.* **37**, 467–477 (2010).
  35. Seibt, U., Rajabi, A., Griffiths, H. & Berry, J. A. Carbon isotopes and water use efficiency: sense and sensitivity. *Oecologia* **155**, 441–454 (2008).
  36. Song, X., Barbour, M. M., Farquhar, G. D., Vann, D. R. & Helliker, B. R. Transpiration rate relates to within- and across-species variations in effective path length in a leaf water model of oxygen isotope enrichment. *Plant. Cell Environ.* **36**, 1338–1351 (2013).
  37. Kahmen, A., Simonin, K., Tu, K., Goldsmith, G. R. & Dawson, T. E. The influence of species and growing conditions on the  $^{18}\text{O}$  enrichment of leaf water and its impact on ‘effective path length’. *N. Phytol.* **184**, 619–630 (2009).
  38. Wang, X. F., Yakir, D. & Avishai, M. Non-climatic variations in the oxygen isotopic compositions of plants. *Glob. Chang. Biol.* **4**, 835–849 (1998).
  39. Cornwell, W. K. et al. Climate and soils together regulate photosynthetic carbon isotope discrimination within  $\text{C}_3$  plants worldwide. *Glob. Ecol. Biogeogr.* **27**, 1056–1067 (2018).
  40. Jiao, W. et al. Observed increasing water constraint on vegetation growth over the last three decades. *Nat. Commun.* **12**, 1–9 (2021).
  41. Liu, L. et al. Soil moisture dominates dryness stress on ecosystem production globally. *Nat. Commun.* **11**, 1–9 (2020).
  42. Hernandez-Santana, V., Rodríguez-Dominguez, C. M., Sebastian-Azcona, J., Perez-Romero, L. F. & Diaz-Espejo, A. Role of hydraulic traits in stomatal regulation of transpiration under different vapour pressure deficits across five Mediterranean tree crops. *J. Exp. Bot.* **74**, 4597–4612 (2023).
  43. Schenk, H. J. & Jackson, R. B. Rooting depths, lateral root spreads and below-ground/above-ground allometries of plants in water-limited ecosystems. *J. Ecol.* **90**, 480–494 (2002).
  44. Ogle, K., Wolpert, R. L. & Reynolds, J. F. Reconstructing plant root area and water uptake profiles. *Ecology* **85**, 1967–1978 (2004).
  45. Ward, D., Wiegand, K. & Getzin, S. Walter’s two-layer hypothesis revisited: back to the roots! *Oecologia* **172**, 617–630 (2013).
  46. Isbell, F. et al. Biodiversity increases the resistance of ecosystem productivity to climate extremes. *Nature* **526**, 574–577 (2015).
  47. Urgoiti, J. et al. No complementarity no gain—Net diversity effects on tree productivity occur once complementarity emerges during early stand development. *Ecol. Lett.* **25**, 851–862 (2022).
  48. Brinkmann, N. et al. Employing stable isotopes to determine the residence times of soil water and the temporal origin of water taken up by *Fagus sylvatica* and *Picea abies* in a temperate forest. *N. Phytol.* **219**, 1300–1313 (2018).
  49. Allen, S. T., Kirchner, J. W., Braun, S., Siegwolf, R. T. W. & Goldsmith, G. R. Seasonal origins of soil water used by trees. *Hydrol. Earth Syst. Sci.* **23**, 1199–1210 (2019).
  50. Goldsmith, G. R., Allen, S. T., Braun, S., Siegwolf, R. T. W. & Kirchner, J. W. Climatic influences on summer use of winter precipitation by trees. *Geophys. Res. Lett.* **49**, e2022GL098323 (2022).
  51. Hahn, W. J., Rempe, D. M., Dralle, D. N., Dawson, T. E. & Dietrich, W. E. Oak transpiration drawn from the weathered bedrock vadose zone in the summer dry season. *Water Resour. Res.* **56**, e2020WR027419 (2020).
  52. Davis, S. D. & Mooney, H. A. Water use patterns of four co-occurring chaparral shrubs. *Oecologia* **70**, 172–177 (1986).
  53. Redtfeldt, R. A. & Davis, S. D. Physiological and morphological evidence of niche segregation between two co-occurring species of *Adenostoma* in California Chaparral. *Ecoscience* **3**, 290–296 (1996).
  54. Schwendenmann, L., Dierick, D., Köhler, M. & Hölscher, D. Can deuterium tracing be used for reliably estimating water use of tropical trees and bamboo? *Tree Physiol.* **30**, 886–900 (2010).
  55. Evaristo, J. et al. Characterizing the fluxes and age distribution of soil water, plant water, and deep percolation in a model tropical ecosystem. *Water Resour. Res.* **55**, 3307–3327 (2019).
  56. von Freyberg, J., Allen, S. T., Grossiord, C. & Dawson, T. E. Plant and root-zone water isotopes are difficult to measure, explain, and predict: some practical recommendations for determining plant water sources. *Methods Ecol. Evol.* **11**, 1352–1367 (2020).
  57. Bernhard, F. et al. Tree- and stand-scale variability of xylem water stable isotope signatures in mature beech, oak and spruce. *Ecohydrology* **17**, 1–20 (2024).
  58. de Deurwaerder, H. P. T. et al. Causes and consequences of pronounced variation in the isotope composition of plant xylem water. *Biogeosciences* **17**, 4853–4870 (2020).
  59. Magh, R. K. et al. Competition for water rather than facilitation in mixed beech-fir forests after drying-wetting cycle. *J. Hydrol.* **587**, 124944 (2020).
  60. Marshall, J. D., Cuntz, M., Beyer, M., Dubbert, M. & Kuehnhammer, K. Borehole equilibration: testing a new method to monitor the isotopic composition of tree xylem water in situ. *Front. Plant Sci.* **11**, 1–14 (2020).
  61. Mennekes, D., Rinderer, M., Seeger, S. & Orlowski, N. Ecophysiological travel times derived from in situ stable water isotope measurements in trees during a semi-controlled pot experiment. *Hydrol. Earth Syst. Sci.* **25**, 4513–4530 (2021).
  62. Jacobsen, A. L., Pratt, R. B., Davis, S. D. & Ewers, F. W. Comparative community physiology: Nonconvergence in water relations among three semi-arid shrub communities. *N. Phytol.* **180**, 100–113 (2008).

63. Cohen, Y., Cohen, S., Cantuarias-Aviles, T. & Schiller, G. Variations in the radial gradient of sap velocity in trunks of forest and fruit trees. *Plant Soil* **305**, 49–59 (2008).
64. Seeger, S. & Weiler, M. Temporal dynamics of tree xylem water isotopes: In situ monitoring and modeling. *Biogeosciences* **18**, 4603–4627 (2021).
65. Guerrieri, R. et al. Disentangling the role of photosynthesis and stomatal conductance on rising forest water-use efficiency. *Proc. Natl. Acad. Sci. USA* **116**, 16909–16914 (2019).
66. Mathias, J. M. & Thomas, R. B. Global tree intrinsic water use efficiency is enhanced by increased atmospheric CO<sub>2</sub> and modulated by climate and plant functional types. *Proc. Natl. Acad. Sci. USA* **118**, e2014286118 (2021).
67. Henry, C. et al. A stomatal safety-efficiency trade-off constrains responses to leaf dehydration. *Nat. Commun.* **10**, 1–9 (2019).
68. Hu, Y. et al. Woody species with higher hydraulic efficiency or lower photosynthetic capacity discriminate more against <sup>13</sup>C at the global scale. *Sci. Total Environ.* **908**, 168172 (2024).
69. Mencuccini, M. et al. Leaf economics and plant hydraulics drive leaf: wood area ratios. *N. Phytol.* **224**, 1544–1556 (2019).
70. Ryel, R. J., Ivans, C. Y., Peek, M. S. & Leffler, A. J. Functional differences in soil water pools: a new perspective on plant water use in water-limited ecosystems. in *Progress in Botany* 397–422. [https://doi.org/10.1007/978-3-540-72954-9\\_16](https://doi.org/10.1007/978-3-540-72954-9_16) (2008).
71. McDowell, N. G. & Allen, C. D. Darcy's law predicts widespread forest mortality under climate warming. *Nat. Clim. Change* **5**, 669–672 (2015).
72. Medrano, H., Flexas, J. & Galmés, J. Variability in water use efficiency at the leaf level among Mediterranean plants with different growth forms. *Plant Soil* **317**, 17–29 (2009).
73. Máguas, C. et al. Responses of woody species to spatial and temporal ground water changes in coastal sand dune systems. *Biogeosciences* **8**, 3823–3832 (2011).
74. Mueller, K. E., Kray, J. A. & Blumenthal, D. M. Coordination of leaf, root, and seed traits shows the importance of whole plant economics in two semiarid grasslands. *N. Phytol.* **241**, 2410–2422 (2024).
75. Blanco-Sánchez, M. et al. Natural selection favours drought escape and an acquisitive resource-use strategy in semi-arid Mediterranean shrubs. *Funct. Ecol.* **36**, 2289–2302 (2022).
76. Nardini, A., Battistuzzo, M. & Savi, T. Shoot desiccation and hydraulic failure in temperate woody angiosperms during an extreme summer drought. *N. Phytol.* **200**, 322–329 (2013).
77. Oliveira, R. S. et al. Linking plant hydraulics and the fast-slow continuum to understand resilience to drought in tropical ecosystems. *N. Phytol.* **230**, 904–923 (2021).
78. López, R., Cano, F. J., Martin-StPaul, N. K., Cochard, H. & Choat, B. Coordination of stem and leaf traits define different strategies to regulate water loss and tolerance ranges to aridity. *N. Phytol.* **230**, 497–509 (2021).
79. Abatzoglou, J. T., Dobrowski, S. Z., Parks, S. A. & Hegewisch, K. C. TerraClimate, a high-resolution global dataset of monthly climate and climatic water balance from 1958–2015. *Sci. Data* **5**, 1–12 (2018).
80. Rodríguez-Fernández, J. L. et al. Mapa Geológico de España y Portugal a escala 1:1.000.000. *IGME*. [https://info.igme.es/cartografiadigital/datos/geologicos1M/Geologico1000\\_2015/pdfs/EditadoG1000\\_2015.pdf](https://info.igme.es/cartografiadigital/datos/geologicos1M/Geologico1000_2015/pdfs/EditadoG1000_2015.pdf) (2015).
81. Raunkiaer, C. *The Life Forms of Plants and Statistical Plant Geography Being the Collected Papers of C. Raunkiaer*. (Clarendon Press, 1934).
82. de la Riva, E. G. et al. Relationships between leaf mass per area and nutrient concentrations in 98 Mediterranean woody species are determined by phylogeny, habitat and leaf habit. *Trees Struct. Funct.* **32**, 497–510 (2018).
83. Navarro, T., Pascual, V., Cabezudo, B. & Alados, C. Architecture and functional traits of semi-arid shrub species in Cabo de Gata Natural Park, se Spain. *Candollea* **64**, 69–84 (2009).
84. Gavilán, R. G., Vilches, B., Gutiérrez-Girón, A., Blanquer, J. M. & Escudero, A. Sclerophyllous Versus Deciduous Forests in the Iberian Peninsula: A Standard Case of Mediterranean Climatic Vegetation Distribution. in *Geographical Changes in Vegetation and Plant Functional Types* (eds. Grellier, A. et al.) 101–116. [https://doi.org/10.1007/978-3-319-68738-4\\_5](https://doi.org/10.1007/978-3-319-68738-4_5) (Springer, Cham, 2018).
85. Beccari, E. & Carmona, C. P. Aboveground and belowground sizes are aligned in the unified spectrum of plant form and function. *Nat. Commun.* <https://doi.org/10.1038/s41467-024-53180-x> (2024).
86. Schwinning, S. The water relations of two evergreen tree species in a karst savanna. *Oecologia* **158**, 373–383 (2008).
87. Ehleringer, J. R. & Osmond, C. B. Stable isotopes. *Plant Physiol. Ecol.* 281–300. [https://doi.org/10.1007/978-94-009-2221-1\\_13](https://doi.org/10.1007/978-94-009-2221-1_13) (1989).
88. Diaz-Teijeiro, M. F., Rodríguez-Arévalo, J. & Castaño, S. La Red Española de Vigilancia de Isótopos en la Precipitación (REVIP): distribución isotópica espacial y aportación al conocimiento del ciclo hidrológico. *Ing. Civ.* **155**, 87–97 (2009).
89. León-Sánchez, L., Nicolás, E., Nortes, P. A., Maestre, F. T. & Querjeto, J. I. Photosynthesis and growth reduction with warming are driven by nonstomatal limitations in a Mediterranean semi-arid shrub. *Ecol. Evol.* **6**, 2725–2738 (2016).
90. Cernusak, L. A. et al. Environmental and physiological determinants of carbon isotope discrimination in terrestrial plants. *N. Phytol.* **200**, 950–965 (2013).
91. Pivovarov, A. L. et al. Hydraulic architecture explains species moisture dependency but not mortality rates across a tropical rainfall gradient. *Biotropica* **53**, 1213–1225 (2021).
92. Adobe Inc. Adobe Photoshop (22.5.0). <https://www.adobe.com/es/products/photoshop.html> (2021).
93. Bowen, G. J., Wassenaar, L. I. & Hobson, K. A. Global application of stable hydrogen and oxygen isotopes to wildlife forensics. *Oecologia* **143**, 337–348 (2005).
94. Bowen, G. J. & Revenaugh, J. Interpolating the isotopic composition of modern meteoric precipitation. *Water Resour. Res.* **39**, 1299 (2003).
95. Stock, B. C. et al. Analyzing mixing systems using a new generation of Bayesian tracer mixing models. *PeerJ* **2018**, 1–27 (2018).
96. Barbeta, A. et al. An explanation for the isotopic offset between soil and stem water in a temperate tree species. *N. Phytol.* **227**, 766–779 (2020).
97. Stock, B. C. & Semmens, B. X. MixSIAR GUI user manual: Version 1.0. 1–42 (2013).
98. Hoffman, G. E. & Schadt, E. E. variancePartition: interpreting drivers of variation in complex gene expression studies. *BMC Bioinformatics* **17**, 483 (2016).
99. Münkemüller, T. et al. How to measure and test phylogenetic signal. *Methods Ecol. Evol.* **3**, 743–756 (2012).
100. Ives, A. R. & Helmus, M. R. Generalized linear mixed models for phylogenetic analyses of community structure. *Ecol. Monogr.* **81**, 511–525 (2011).
101. Smith, S. A. & Brown, J. W. Constructing a broadly inclusive seed plant phylogeny. *Am. J. Bot.* **105**, 302–314 (2018).
102. Zanne, A. E. et al. Three keys to the radiation of angiosperms into freezing environments. *Nature* **506**, 89–92 (2014).
103. R Core Team. *R: A Language and Environment for Statistical Computing* (R Core Team, 2023).
104. Pinheiro, J., Bates, R Core Team. nlme: Linear and Nonlinear Mixed Effects Models. R package version 3.1-168. <https://CRAN.R-project.org/package=nlme> (2025).
105. Li, D., Dinnage, R., Nell, L. A., Helmus, M. R. & Ives, A. R. phyr: An r package for phylogenetic species-distribution modelling in ecological communities. *Methods Ecol. Evol.* **11**, 1455–1463 (2020).
106. Jin, Y. & Qian, H. V. PhylMaker: an R package that can generate very large phylogenies for vascular plants. *Ecography* **42**, 1353–1359 (2019).

107. Stock, B. & Semmens, B. MixSIAR GUI User Manual. Version 3.1. <https://doi.org/10.5281/zenodo.1209993>.
108. Kohn, M. J. Carbon isotope compositions of terrestrial C3 plants as indicators of (paleo)ecology and (paleo)climate. *Proc. Natl Acad. Sci. USA* **107**, 19691–19695 (2010).
109. Castroviejo, S. Flora Ibérica. *Real Jard. Botánico, CSIC, Madrid* **1–8**, 10–15,

## Acknowledgements

The authors wish to thank María José Espinosa for invaluable help with sample processing and laboratory work over the years. This study was funded by the Fundación Séneca de la Región de Murcia (grant 20654/JLI/18 awarded to I.P.) and the Ministry of Science of Spain (grants PID2019-107382RB-I00, PID2022-141041NB-I00, CGL2013-48753-R, AGL-2006-11234 awarded to J.I.Q.). I.P. also acknowledges funding from a Ramón y Cajal project and contract (RYC2021-033081-I) funded by the Ministry of Science and Innovation and co-funded by the European Union-Next Generation Plan funded by European Union-NextGenerationEU. J.I.Q. acknowledges funding from AGROALNEXT (PRTR-C17.I1), supported by MCIN with funding from NextGenerationEU.

## Author contributions

I.P. and J.I.Q. conceived the study and obtained funding; I.P., J.I.Q., F.M.G., C.M.G., W.R. and E.G.R. performed field work; I.P., F.M.G., C.M.G. and W.R. conducted laboratory work; F.M.G., I.P. and J.I.Q. conducted statistical analyses and interpreted the data; F.M.G., J.I.Q. and I.P. wrote the manuscript with input from all co-authors.

## Competing interests

The authors declare no competing interests.

## Additional information

**Supplementary information** The online version contains supplementary material available at <https://doi.org/10.1038/s41467-025-59348-3>.

**Correspondence** and requests for materials should be addressed to José I. Querejeta.

**Peer review information** *Nature Communications* thanks James Ehleringer and the other, anonymous, reviewer(s) for their contribution to the peer review of this work. A peer review file is available.

**Reprints and permissions information** is available at <http://www.nature.com/reprints>

**Publisher's note** Springer Nature remains neutral with regard to jurisdictional claims in published maps and institutional affiliations.

**Open Access** This article is licensed under a Creative Commons Attribution-NonCommercial-NoDerivatives 4.0 International License, which permits any non-commercial use, sharing, distribution and reproduction in any medium or format, as long as you give appropriate credit to the original author(s) and the source, provide a link to the Creative Commons licence, and indicate if you modified the licensed material. You do not have permission under this licence to share adapted material derived from this article or parts of it. The images or other third party material in this article are included in the article's Creative Commons licence, unless indicated otherwise in a credit line to the material. If material is not included in the article's Creative Commons licence and your intended use is not permitted by statutory regulation or exceeds the permitted use, you will need to obtain permission directly from the copyright holder. To view a copy of this licence, visit <http://creativecommons.org/licenses/by-nc-nd/4.0/>.

© The Author(s) 2025